

AD \_\_\_\_\_

USAARL REPORT NO. 74-6

THE EFFECTS OF INITIAL SPINAL CONFIGURATION  
ON PILOT EJECTION

October 1973

U. S. ARMY AEROMEDICAL RESEARCH LABORATORY

Fort Rucker, Alabama 36360



AD \_\_\_\_\_

USAARL REPORT NO. 74-6

THE EFFECTS OF INITIAL SPINAL CONFIGURATION  
ON PILOT EJECTION

By

Y. King Liu, Ph.D., Consultant  
U. S. Army Aeromedical Research Laboratory

Uwe R. Pontius, M. S.  
Ronald R. Hosey, M. S.

Tulane University School of Medicine  
New Orleans, LA 70112

October 1973

U. S. ARMY AEROMEDICAL RESEARCH LABORATORY

Fort Rucker, Alabama

U. S. Army Medical Research and Development Command

Distribution Statement

This document has been approved for public release and sale; its  
distribution is unlimited.

## NOTICE

Qualified requesters may obtain copies from the Defense Documentation Center (DDC), Cameron Station, Alexandria, Virginia. Orders will be expedited if placed through the librarian or other person designated to request documents from DDC (Formerly ASTIA).

### Change of Address

Organization receiving reports from the US Army Aeromedical Research Laboratory on automatic mailing lists should confirm correct address when corresponding about laboratory reports.

### Disposition

Destroy this report when it is no longer needed. Do not return it to the originator.

### Distribution Statement

This document has been approved for public release and sale; its distribution is unlimited.

### Disclaimer

The findings in this report are not to be construed as an official Department of the Army position unless so designated by other authorized documents.

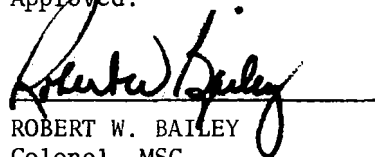
FOREWORD

This report was submitted to the U.S. Army Aeromedical Research Laboratory in fulfillment of Contract No. DABCO1-73-C-0168.

ABSTRACT

The effect of initial spinal alignment on the location and magnitude of maximum vertebral stress during ejection was studied using the Orne-Liu discrete parameter model of the spine. Face curtain, shoulder harness, and seat back restraints were added to the model as linear springs. Spinal alignment data used were from x-rays of 5th, 40th and 95th percentile (sitting height) men seated in the MK-J5(D) ejection seat under static conditions. Maximum normal stresses were shown to occur at L1(5th), T12(40th) and T9(95th) with face curtain and shoulder harness restraint. These locations correspond almost exactly to the predictions of injury based on static observations of the curvature of the initial configuration of the pilot's spine. Inclusion of posterior-anterior seat back support decreased maximum stresses as did the use of an improved lumbar pad which placed the lower spinal column in extension. Failure to utilize the face curtain restraint gave rise to large normal stresses in the upper thoracic column. Results indicated that a state of nearly uniform axial stress exists in the column during ejection and thus the location of maximum bending stress dictates the spinal location of maximum normal stress. Hence, initial spinal alignment, in terms of the curvature of the column, is a major determinant of the location and magnitude of maximum normal stress for a given set of restraints.

Approved:



ROBERT W. BAILEY  
Colonel, MSC  
Commander

TABLE OF CONTENTS

	PAGE
ABSTRACT	
LIST OF FIGURES	
LIST OF TABLES	
INTRODUCTION	1
MK-J5 EJECTION SYSTEM	6
ORNE-LIU MODEL WITH CONSTRAINTS	9
BIOMECHANICAL DATA	14
RESULTS AND DISCUSSION	16
CONCLUSIONS	41
RECOMMENDATIONS	42
REFERENCES	43

LIST OF TABLES

<u>TABLE</u>	<u>PAGE</u>
1. Predicted Fracture Levels (Taken from Kaplan)	9
2. Inertial Distribution Regression Parameters	14
3. 5th Percentile Anthropometric Data	18
4. 40th Percentile Anthropometric Data	19
5. 95th Percentile Anthropometric Data	20
6. Model Configurations	22
7. Test Results	40

LIST OF FIGURES

FIGURE NO.		PAGE
1.	Martin-Baker Acceleration Pulse	2
2.	Spinal Injury Statistics: Moffatt and Howard	2
3.	Spinal Injury Statistics: Delahaye	3
4.	Locations of Multiple Fractures: Delahaye	3
5.	Simplified Spinal Model (Taken from Vulcan and King)	5
6.	MK-J5(A,B) Ejection System (Taken from Kaplan)	7
7.	MK-J5(D) Ejection System (Taken from Kaplan)	8
8.	Views of the Vertebral Column (Modified from Grant's <u>Anatomy</u> )	10
9.	Orne-Liu Discrete Parameter Model of the Spinal Column	11
10.	Free-Body Diagram of Vertebral Body	11
11.	Spinal Alignment, 40th Percentile Aviator (Taken from Kaplan)	15
12.	Center of Gravity of Aviator's Helmet	17
13.	MK-J5(D) Acceleration Pulse with Trapezoidal Idealization	21
14.	Spinal Alignment, 5th Percentile, Position 1, Unrestrained	21
15.	Maximum Normal Stress, 5th Percentile, Position 1, Unrestrained	24
16.	Maximum Axial Forces and Stresses, 5th Percentile, Position 1, Unrestrained	24
17.	Time History of Axial Force, Shear Force, and Bending Moment on Superior Surface of L1, 5th Percentile, Position 1, Unrestrained	25
18.	Axial Force and Bending Moment Distribution at 170 ms, 5th Percentile, Position 1, Unrestrained	25

LIST OF FIGURES (Continued)

<u>FIGURE NO.</u>		<u>PAGE</u>
19.	Spinal Alignment, 5th, 40th, 95th Percentile, Position 1, Face Curtain, Shoulder Harness	26
20.	Maximum Normal Stress, 5th, 40th, 95th Percentile, Position 1, Face Curtain, Shoulder Harness	27
21.	Maximum Axial Force and Bending Moment Distribution, 5th Percentile, Position 1, Face Curtain, Shoulder Harness	28
22.	Time History of Axial Force, Shear Force, and Bending Moment of Superior Surface of L1, 5th Percentile, Position 1, Face Curtain, Shoulder Harness	28
23.	Face Curtain Force, 5th Percentile, Position 1, Face Curtain, Shoulder Harness	29
24.	Spinal Alignment, 5th, 40th, 95th Percentile, Position 1, Face Curtain, Shoulder Harness, Seat Back	31
25.	Maximum Normal Stress, 5th, 40th, 95th Percentile, Position 1, Face Curtain, Shoulder Harness, Seat Back	32
26.	Maximum Axial Forces and Stresses, 5th, 40th, 95th Percentile, Position 1, Face Curtain, Shoulder Harness, Seat Back	33
27.	Time History of Axial Force, Shearing Force and Bending Moment on Superior Surface of L2, 5th Percentile, Position 1, Face Curtain, Shoulder Harness, Seat Back	34
28.	Spinal Alignment, 5th Percentile, Position 2, Shoulder Harness, Seat Back	34
29.	Maximum Normal Stress, 5th Percentile, Position 2, Shoulder Harness, Seat Back	35
30.	Time History of Axial Force, Shearing Force, and Bending Moment on Superior Surface of T7, 5th Percentile, Position 2, Shoulder Harness, Seat Back	35

1

LIST OF FIGURES (Continued)

<u>FIGURE NO.</u>		<u>PAGE</u>
31.	Maximum Axial Force and Bending Moment, 5th Percentile, Position 2, Shoulder Harness, Seat Back	36
32.	Spinal Alignment, 5th Percentile, McDonnell Lumbar Pad, Face Curtain, Shoulder Harness, Seat Back	36
33.	Maximum Normal Stress, 5th Percentile, Face Curtain, Shoulder Harness, Seat Back, McDonnell Lumbar Pad	38
34.	Time History of Axial Force, Shearing Force, and Bending Moment on Superior Surface of T7, 5th Percentile, Position 1, Face Curtain, Shoulder Harness, Seat Back, McDonnell Lumbar Pad	38
35.	Axial Forces and Bending Moments at T = 150 ms, 5th Percentile, Position 1, Face Curtain, Shoulder Harness, Seat Back, McDonnell Lumbar Pad	39

## INTRODUCTION

The advent of high speed and performance aircraft during the early 1940's necessitated the development of powered pilot extraction systems. The ejection systems are capable of separating a man from an aircraft without his striking the vertical stabilizer and attaining sufficient height to allow parachute deployment during low level ejection. In order to accomplish this during the stroke length of the ejection device, the man-seat unit must be subjected to a relatively high amplitude, short duration acceleration pulse (Figure 1). Unfortunately, this generates large forces and deformations in the spinal column which sometimes may exceed safe levels as is evidenced by the large number of vertebral fractures which have been reported following ejection.

Moffatt and Howard (1968) made an extensive compilation of U.S. Air Force and Navy aircraft ejections during the period 1959-1967. They found that 17% of the ejections resulted in vertebral fractures with most (70%) occurring in the lower thoracic region (T7 through T12) (Figure 2). Shannon (1970) studied 561 combatant and noncombatant ejections which occurred during 1967 and 1968. In this study, 8.5% of the ejectees demonstrated vertebral fractures which were caused entirely by the ejection system. Again the lower thoracic and upper lumbar regions were found to be the prime injury sites.

At a recent (1973) Ejection Seat Committee meeting of AGARD, the continuing seriousness of the ejection problem was reported by Prof. R. P. Delahaye of France on behalf of all the participating NATO countries. These included the British, Hellenic, Italian, German and French Air Forces. The U.S. was represented by statistics from the Army and Air Force, but not the Navy. Of 678 ejection episodes in 1972, there were 114 deaths; 98 pilots sustained spinal injuries, which resulted in 160 vertebral fractures. The distribution of 160 fractures in 98 pilots is shown in Figure 3. Figure 4 shows the distribution of fractures in pilots with multiple spinal fractures. Figures 3 and 4 show the greatest incidence of injury to be at T7 - T8 and at T12 - L1, the thoracolumbar transition vertebra. Prof. Delahaye further stated that the frequency of multiple fractures was increasing. There exists a general consensus that poor initial configuration is the principle cause of fracture, and that this has been proven convincingly through the use of the powered inertial reel in the German Air Force. With respect to anthropomorphic type, he reported that "thin and tall" pilots have higher frequency of fracture in the T7 - T8 region, while "stout and medium" pilots tend to have T12 - L1 fractures.

In addition to the medical aspects, there is a substantial economic cost associated with unnecessary fracture. Ewing (1971) calculated an average yearly cost to the U.S. Navy of \$6,797,718 for aviators who had sustained vertebral fractures.

Latham (1957) was one of the first investigators to correlate vertebral fracture with the biomechanics of the spinal column. He

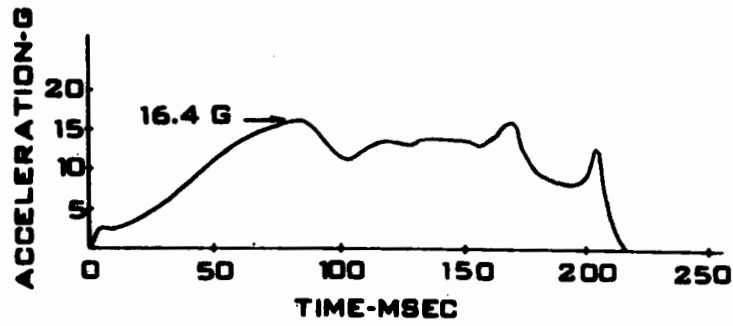


Figure 1. Martin-Baker Acceleration Pulse

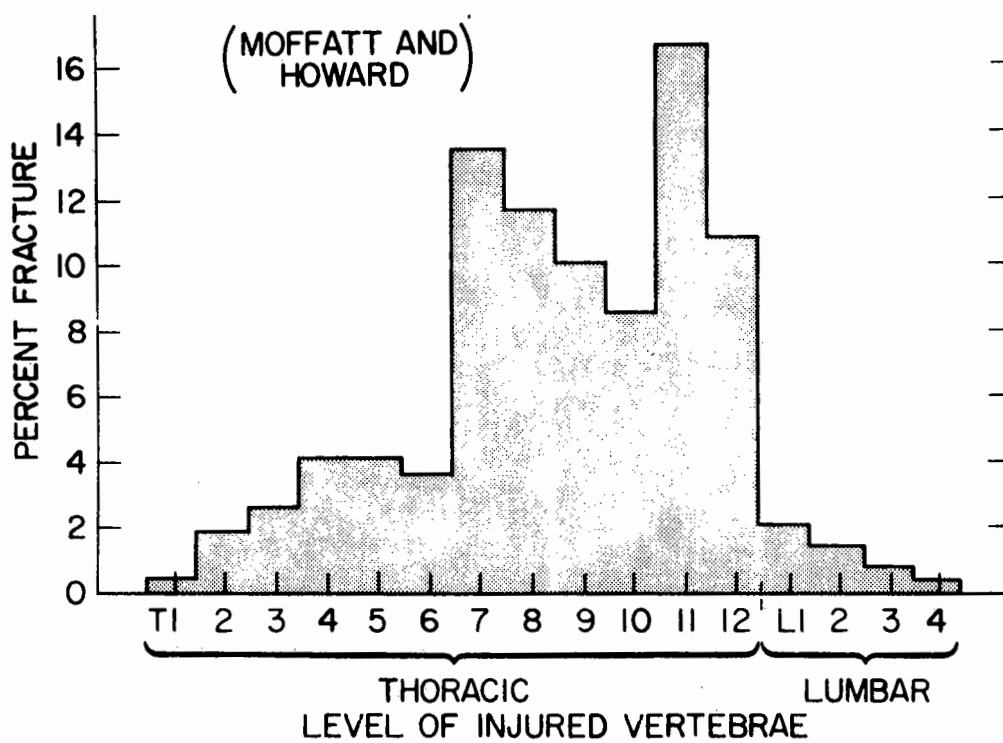


Figure 2. Spinal Injury Statistics:  
Moffatt and Howard

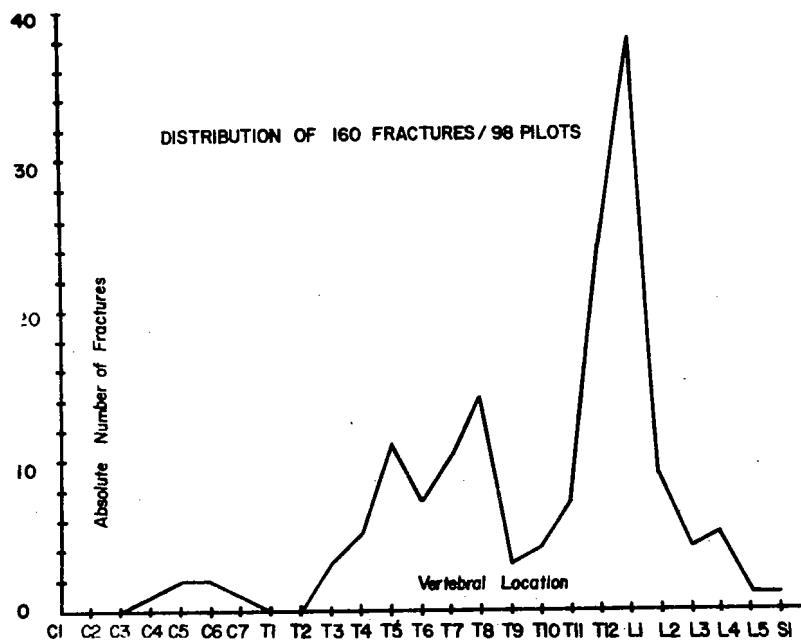


Figure 3. Spinal Injury Statistics: Delahaye

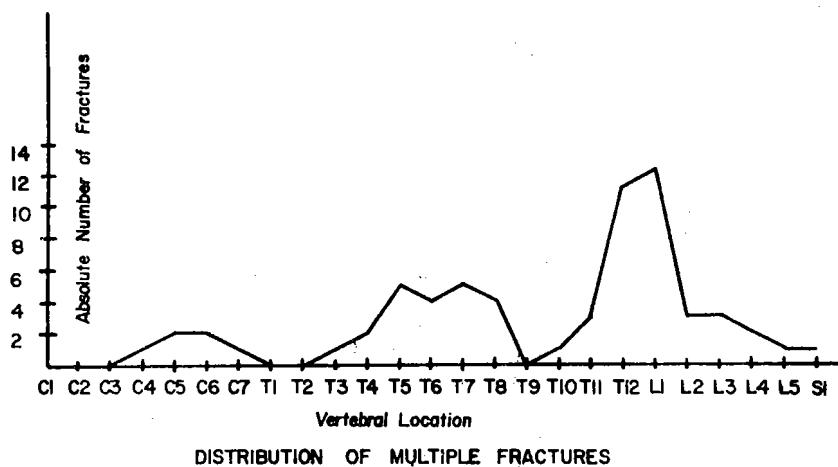


Figure 4. Locations of Multiple Fractures: Delahaye

reported on work done by the German Air Force during the early 40's which ascribed anterior fractures of the vertebrae to excessive flexion of the trunk. Additionally, he noted the need for a lumbar pad to attain correct spinal alignment prior to ejection and the increased bending induced by the rearward rotation of the thrust axis relative to the geometric axis of the spine. Bosee and Payne (1961) studied the Martin-Baker ejection system. They postulated that the common anterior lip fracture was due to bending stresses which could be induced by poor initial spinal alignment. This hypothesis was later corroborated experimentally by Vulcan et al. (1970). They attached strain gages to cadaver vertebrae and demonstrated the existence of large compressive stresses on the anterior edge of the vertebral body.

Mathematical models have also been employed to study the vertebral fracture problem. Early models were derived to study only axial deformation. Latham (1957) modelled the man, ejection seat, spine configuration as a single spring-mass system. Unfortunately, the use of a single spring for the spine prevents any study of regional spinal failures, e.g., the propensity of lower thoracic and upper lumbar fracture noted earlier. This deficiency was somewhat rectified by Toth (1967) who used eight spring, mass elements to study the T11-pelvis segment. However, the model was still confined to a study of axial deformations.

Vulcan and King (1970) used a three mass model to study the effect of harness and seat back constraints (Figure 5). The force levels at the lower vertebral levels were determined by changing the dimensions and mass of the torso unit to correspond to different spinal levels. Again it was found that large bending and axial forces existed in the lower thoracic and upper lumbar spine.

Orne and Liu (1971) have derived the most comprehensive model of the spinal column presently available. This model consists of a series of rigid masses connected by viscoelastic, massless beams. This formulation rectified most of the earlier shortcomings by accounting for axial, shear, and bending deformations of the spinal column, the variable size of vertebrae and discs, the natural curvature of the spine, and the eccentric inertial loading on the spine produced by the mass of the head and trunk. A study of a typical unrestrained ejection sequence with this model indicated that large anterior stresses did exist in the lower thoracic and upper lumbar regions if the stresses due to axial and bending forces were combined according to the strength of materials formula,  $\sigma = P/A \pm Mc/I$ . A serious shortcoming of this model, however, was the fact that it did not account for the restraining effect of the shoulder harness and/or seat back.

The purpose of the present investigation was to extend the Orne-Liu model by including the effects of external constraints. This was accomplished and the model used to study the effects of initial curvature on spinal injury potential of the MK-J5(D) ejection system.

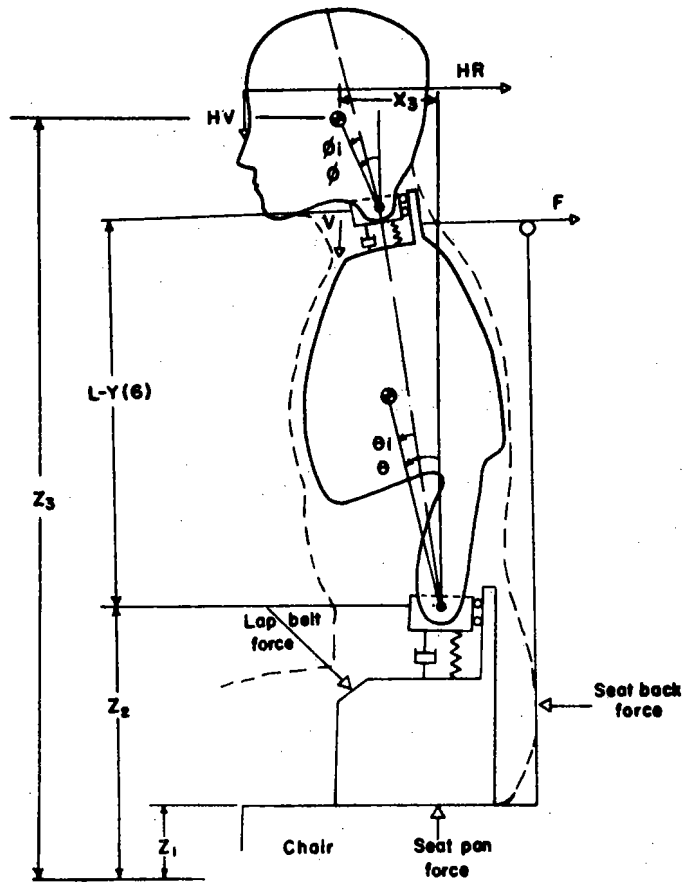


Figure 5. Simplified Spinal Model  
(Taken from Vulcan & King)

### MK-J5 EJECTION SYSTEM

The separation of the aviator from the cockpit is accomplished by the Model MK-J5 ejection seat shown in Figure 6. The MK-J5 is a fully automatic, cartridge operated ejection system which incorporates the following features:

1. A high velocity ejection gun which provides sufficient acceleration to clear the vertical stabilizer and attain sufficient altitude for safe chute deployment during low level ejection.
2. A dual automatic leg restraining mechanism which helps prevent flail injuries to the leg.
3. An integrated back pad and seat pan.
4. A face blind which helps restrain forward head motion.

Despite these features, several shortcomings of the system have been described. Bosee and Payne (1961) and Kaplan (1972) have indicated that the MK-J5(A,B) ejection system forced the aviator into a flexed position in the lower spinal region and also placed the mass of the head and thorax further anterior than would be commensurate with good spinal alignment. This initial configuration would predispose the aviator to spinal fracture. Additionally, Kaplan (1972) indicated that insufficient thigh support could exacerbate flexion in the lumbar region through an induced rotation of the pelvis. He also pointed out the necessity for proper design of the lumbar support pad.

In order to rectify some of these problems, modifications were made to the MK-J5(A,B) system. Kaplan (1972) reported on these changes which are designated the MK-J5(D) system (Figure 7). It was found that comfort had increased through the incorporation of an improved harness system and an elongation of the thigh support. In addition, thoracic flexion was reduced when compared to that of the earlier MK-J5(A,B) system, but certain size percentile aviators were still predisposed to fracture due to improper alignment. Kaplan (1972) notes: "The 5th and 95th percentiles (sitting height) appear to be more predisposed to vertebral fracture than the 40th percentile due to seat back contour design. The face curtain firing position increased vertebral flexion in the 95th percentile."

Kaplan (1972) also analyzed statically the probability of fracture from spinal alignment x-rays taken while 5th, 40th and 95th percentile (sitting height) aviators were seated in the MK-J5(D) system in the face curtain (position 1) or secondary "D" ring position (position 2). A consideration of the spinal alignments indicated that the

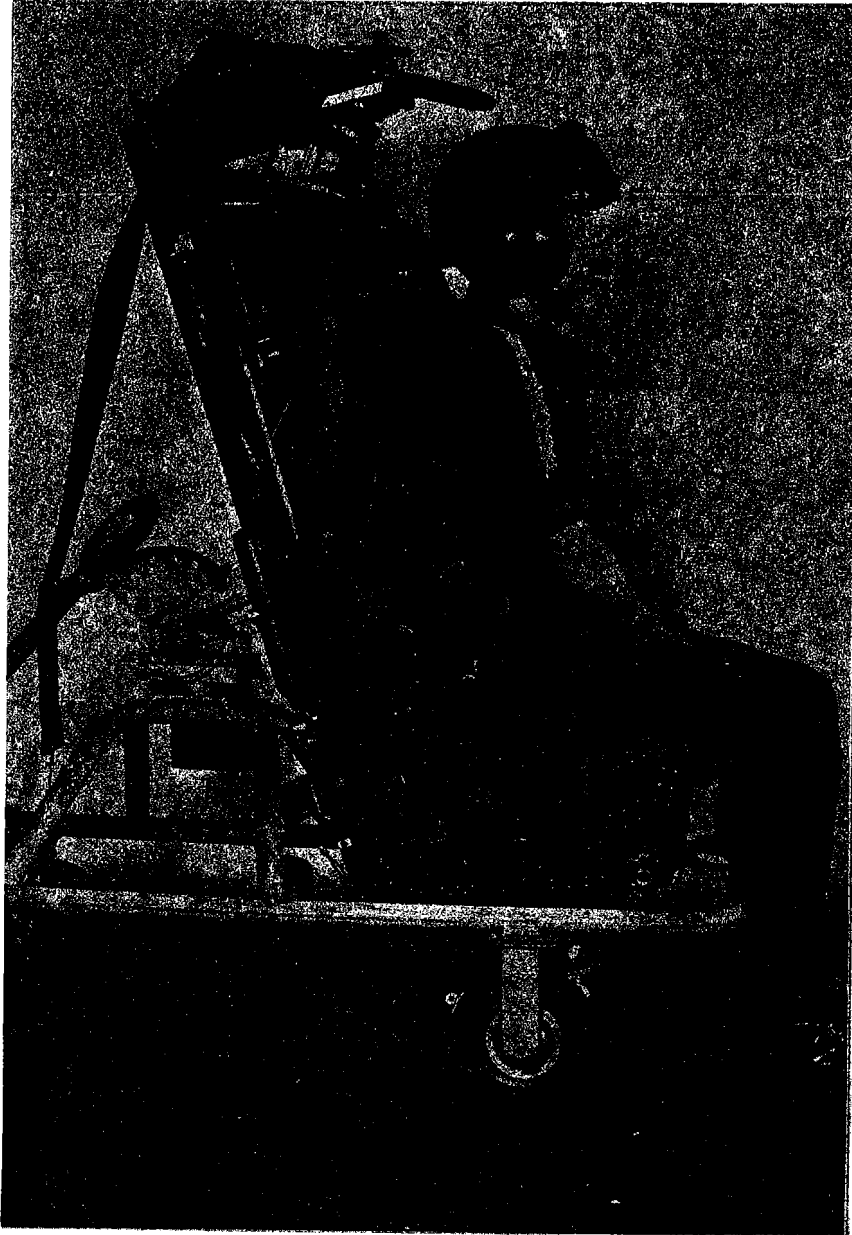


Figure 6. MK-J5(A,B) Ejection System  
(Taken from Kaplan)



Figure 7. MK-J5(D) Ejection System  
(Taken from Kaplan)

probable level of fracture differed with percentile sitting height as given below in Table 1:

TABLE 1

PREDICTED FRACTURE LEVELS, Kaplan (1972)

	Percentile Sitting Height		
	<u>5</u>	<u>40</u>	<u>95</u>
Spinal Level	T12	T9-11	T9

In order to study these statically derived observations under dynamic conditions, the Orne-Liu model of the spinal column, with restraint added, was used to investigate the dynamic response of the spine using data reported by Kaplan (1972).

ORNE-LIU MODEL WITH CONSTRAINTS

The main load carrying component of the human body during ejection is the spinal column (Figure 8). It consists of 33 vertebrae and 23 intervertebral discs. In accordance with their weight bearing functions, the vertebrae and discs increase in size caudally. Regional variations in the shape of these components account for the cervical, thoracic and lumbar curvatures found in the adult spine. The mobility of the spine is primarily due to the flexibility of the intervertebral discs while the limits of motion are defined by ligaments, facets, muscles and bony overlaps. An important consideration in the present investigation is the effect of the ribs in preventing midsagittal flexion of the thoracic column. The relatively stiff, box-like thoracic cage has practically a rigid-body motion relative to the cervical or lumbar spine, i.e., the mobility of the spine in the midsagittal plane is largely confined to the lumbar and cervical regions.

Basing their work on the anatomy of the spine, Orne and Liu (1971) have formulated the most advanced dynamic spinal model now available. The model consists of alternating rigid masses, which represent the inertial properties of the torso, and massless deformable links which account for the elastic properties of the spinal column (Figure 9). This discretization allows the spinal model to account for, simultaneously:

1. the axial, shear and bending deformations of the discs,
2. the variable size of vertebrae and discs,
3. the natural curvature of the spine,
4. the eccentric inertial loading on the spine produced by the mass of the head and trunk.

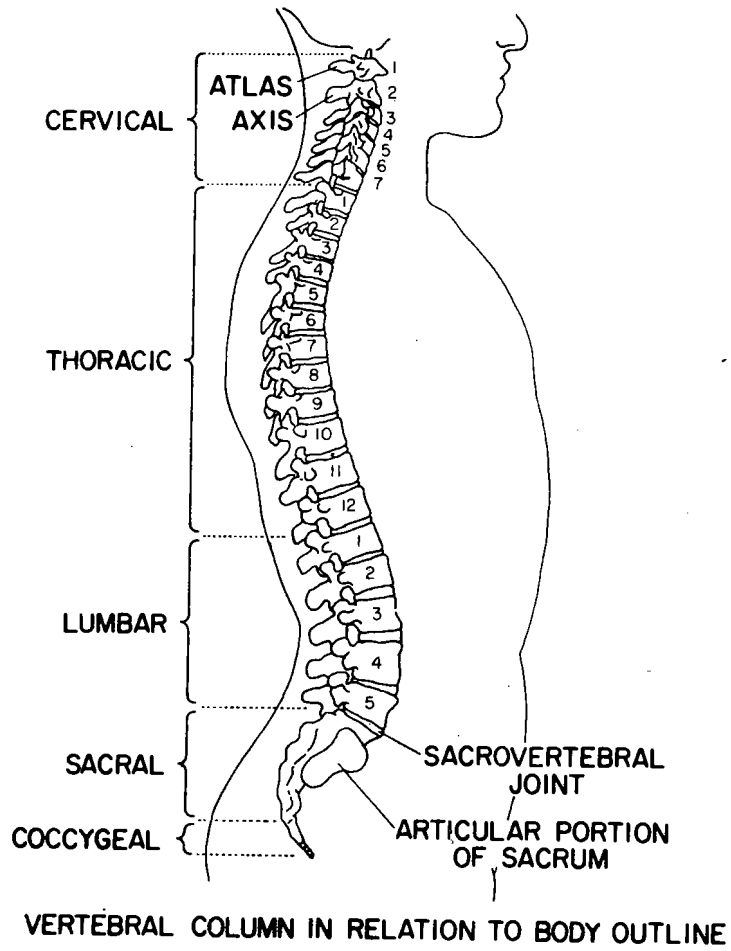


Figure 8. Views of the Vertebral Column  
(Modified from Grant's Anatomy)

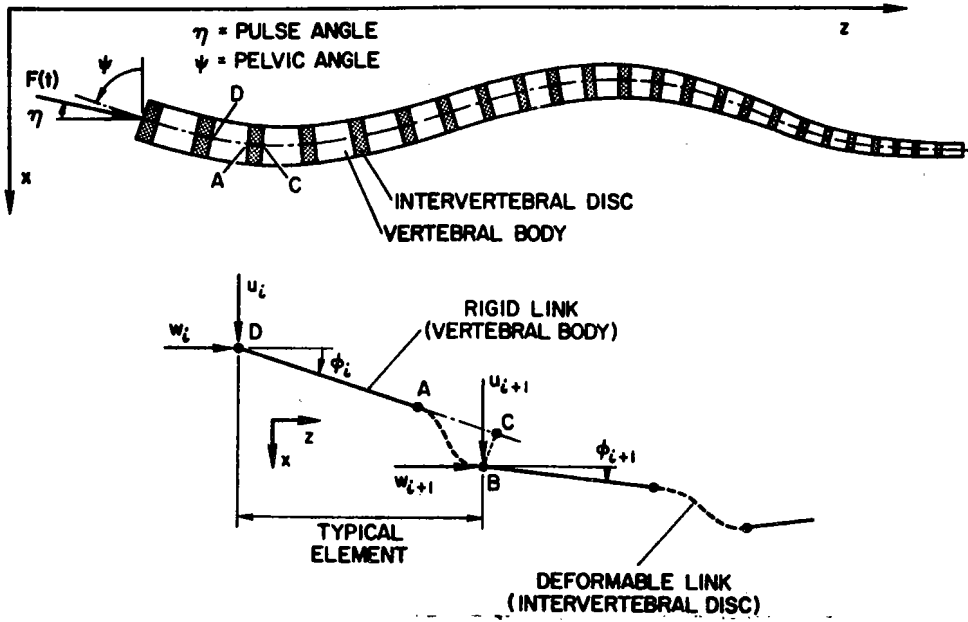


Figure 9. Orne-Liu Discrete Parameter Model of the Spinal Column

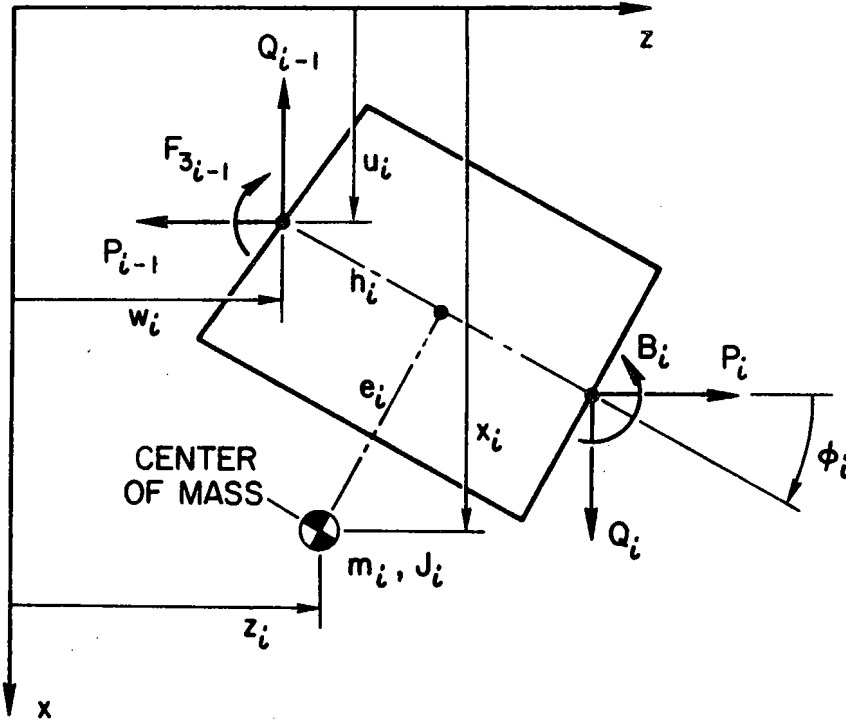


Figure 10. Free-Body Diagram of Vertebral Body

The following equations of motion for the model are given only for the purpose of showing how the constraints are added. Details of the derivation may be found in Orne and Liu (1971). The forces acting on the vertebral body are shown in Figure 10, which is the free-body diagram for a typical vertebral segment. The center of mass,  $m_i$ , has an eccentricity,  $e_i$ , with respect to the vertical axis of the vertebral body.  $J_i$  is the mass moment of inertia about an axis perpendicular to the sagittal plane and through the center of mass and  $h_i$  is one-half the vertebral height. The equations of motion of the vertebrae are:

$$m_i \ddot{x}_i = Q_i - Q_{i-1}$$

and

$$m_i \ddot{z}_i = P_i - P_{i-1}$$

and

$$J_i \ddot{\phi}_i = (F3_{i-1} - B_i) - C_{2i}Q_{i-1} + C_{3i}Q_i + C_{1i}P_{i-1} - C_{4i}P_i$$

where

$$C_{1i} = - (h_i \sin \phi_i + e_i \cos \phi_i)$$

$$C_{2i} = - (h_i \cos \phi_i - e_i \sin \phi_i)$$

$$C_{3i} = h_i \cos \phi_i + e_i \sin \phi_i$$

$$C_{4i} = h_i \sin \phi_i - e_i \cos \phi_i$$

The  $Q_i$ ,  $P_i$ ,  $F3_i$ , and  $B_i$  are the force and moment reactions of the discs on the vertebrae. To these equations must be added the constraining forces of the shoulder harness, face curtain, and seat back. Although the Orne-Liu model can be used to represent each vertebral level as a separate entity, it would unnecessarily complicate the modelling process to discretize the entire column. Thus, the segments T1 to T6 were modelled as a rigid link. This assumption is based on the work of Snyder et al. (1971), who found that the thoracic segments which support the rib cage act as a rigid link insofar as midsagittal bending is concerned. Also, the vast majority of vertebral fractures occur below the level of T6. Additionally, the cervical region was lumped into two segments. One segment contained vertebrae C7 through C4 and the other C3 through C1. Linear springs were used to model the restraining effects of the shoulder harness, face curtain, and seat back. By including the restraining forces the equations of motion change to:

$$m\ddot{x}_i = Q_i - Q_{i-1} - RX_i$$

$$m\ddot{z}_i = P_i - P_{i-1} - RZ_i$$

$$J_i \ddot{\phi}_i = (F_{3i-1} - B_i - MX_i - MZ_i) - C_{2i} Q_{i-1} + C_{3i} Q_i \\ + C_{1i} P_{i-1} - C_{4i} P_i$$

where

$$RX_i = k_x (u_i - u_{i0} + d_i \sin \phi_i - d_i \sin \phi_{i0})$$

$$RZ_i = k_z (w_i - w_{i0} + d_i \cos \phi_i - d_i \cos \phi_{i0})$$

$$MX_i = -RX_i (C_{2i} + d_i \cos \phi_i)$$

$$MZ_i = RZ_i (C_{1i} + d_i \sin \phi_i)$$

The quantities,  $RX_i$ ,  $RZ_i$ ,  $MX_i$  and  $MZ_i$  are the component force and moment reactions of the restraining springs on the vertebrae,  $d_i$  is the distance along the vertebral axis from the inferior vertebral end plate to the point of attachment of the restraining spring and  $u_i$  and  $w_i$  are the instantaneous configuration co-ordinates. For the seat back and face curtain restraints,  $d_i$  was taken as  $h_i$ , one-half the vertebral height. The shoulder harness springs were attached at the upper and lower ends of the T1 through T6 segment. Thus  $d_i$  was set to  $2h_i$  for the upper harness spring and zero for the lower. The spring constants  $k_x$  and  $k_z$  were selected on the basis of experimental work done by Vulcan and King (1970). Their tests had indicated an effective  $k_x$  of 200 lb/in when the torso displacement and horizontal shoulder strap force were considered. The vertical spring constant  $k_z$  was chosen as 50 lb/in since Vulcan and King (1970) noted an approximately 150 lb decrease in the vertical portion of the shoulder strap. In the absence of information on the effective elasticity of the seat back and face curtain restraint, the shoulder strap spring constants  $k_z$  and  $k_x$  were utilized for these restraining springs as well. These constants appeared to give reasonable results when used in the face curtain firing position. However, when the 5th percentile, secondary "D" ring configuration was analyzed, excessive forward displacement and rotation of the torso took place due to the large forces generated by the free head. Several spring constants were utilized for the shoulder strap until one which would allow only a relatively small lateral displacement of the torso (one or two inches) was found. The spring constant,  $k_x$ , utilized for the shoulder strap with the head free was 1400 lb/in.

One additional restraint was required to account for the forces developed when the head strikes the anterior chest wall. This restraint was modelled as a linear spring which was engaged when the head rotated 45 degrees forward relative to the torso. The spring constant was selected so that the head would not rotate more than 10 degrees further after engaging the spring. The spring constant so chosen was 100 lb/radian.

With these modified equations of motion, the Orne-Liu model was used to study the MK-J5(D) ejection system.

## BIOMECHANICAL DATA

Prior to exercising the constrained Orne-Liu model of the spine, the physical parameters of the model should be specified. For the purpose of this investigation, the material properties assumed by Orne and Liu (1971) for shear, axial and bending behavior of the disc will be used. Thus, the viscoelastic behavior of the intervertebral disc is governed by a single set of material parameters:  $p_1$ ,  $q_0$ ,  $q_1$ , which have the values 0.030 sec, 1100 psi, and 72 psi-sec respectively. The values of  $G$ , the shear modulus, and  $E_b$ , the bending modulus were taken as 2200 psi and 7700 psi respectively. The shape factor,  $\bar{K}$ , normally associated with shear, was taken to be 1.333 (circular cross-section assumed).

The remaining input data was taken and/or derived from the results of Kaplan (1972). The initial values of spinal curvature,  $\phi_{i0}$ , were taken from the spinal alignments of the aviators as seated in the MK-J5(D) seat (Figure 11). It should be noted that the angles reported by Kaplan (1972) were taken with respect to the thrust axis and not the vertical axis. For the MK-J5 seat, the thrust axis is rotated rearward 19 degrees from the vertical. Also, for one case (5th percentile) the lumbar alignments for an improved lumbar support pad described by Sanford and Kellet (1966) were utilized. The vertebral height was taken as the distance between the centers of the vertebral bodies as measured by Kaplan (1972), minus the disc height used by Orne and Liu (1971). The calculation of  $m_i$ ,  $e_i$ , and  $J_i$  was somewhat more complicated. Liu and Wickstrom (1972) reported regression equations for  $m_i$ ,  $e_i$ , and  $J_i$  derived from segmented cadavers. These equations give the inertial property distribution of the human torso in a form that can be used in the Orne-Liu model. However, in order to use the regression equations, the height, weight, breadth and chest depth of the individual are required. Kaplan (1972) reported measurements of height, weight and sitting height. The additional required measures were determined using the percentile data given by Kaplan (1972) and anthropometric measurements collected by Schane et al. (1969). The final regression parameters are given in Table 2.

TABLE 2

### INERTIAL DISTRIBUTION REGRESSION PARAMETERS

Percentile [Sitting Height]	Weight [lbs]	Height [in]	Chest Depth [in]	Hip Breadth [in]
5	144.1	64.3	20.0	31.83
40	172.0	67.9	21.1	33.23
95	189.5	75.5	22.1	34.63

While these parameters define  $m_i$ ,  $e_i$ , and  $J_i$  for the torso, it is not possible to calculate the cervical or head inertial properties from the

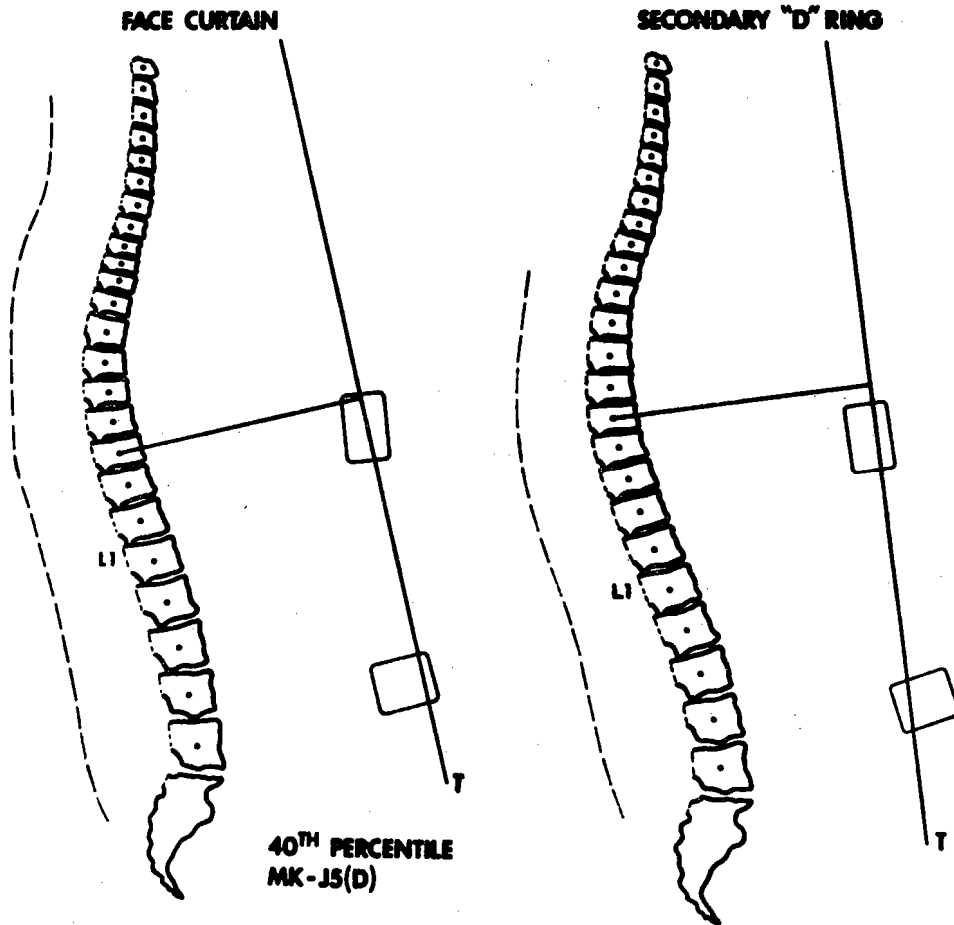


Figure 11. Spinal Alignment, 40th Percentile Aviator (Taken from Kaplan)

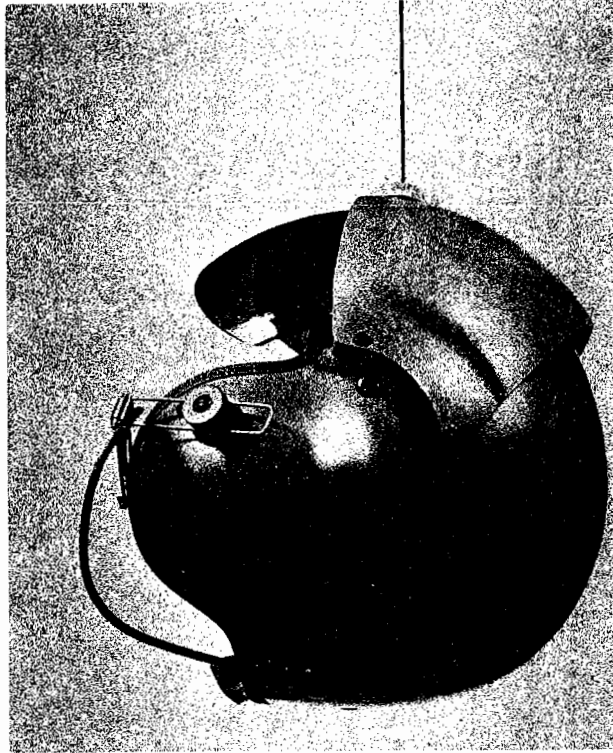
regression equations. Thus, the cervical and head inertial data are taken from Pontius et al. (1972). An additional consideration in the present investigation is the mass of the helmet which is worn by the aviator. The physical properties associated with the helmet were determined by the methods of Walker et al. (1973) and Liu et al. (1971). To find the center of gravity (c.g.) of the helmet, with visor down, it was hung from two points in the midsagittal plane (Figure 12). It was seen that the c.g. of the helmet approximated the location of the c.g. of the head as given by Walker et al. (1973). Thus, it was assumed that the helmet mass (0.088 lb-sec<sup>2</sup>/in) and mass moment of inertia (0.118 lb-sec<sup>2</sup>/in) could simply be added to the respective values for the head.

Using the regression parameter values given in Table 2, the regression equations of Liu and Wickstrom (1972), and the data given in Kaplan (1972), the complete set of input data for the 5th, 40th, and 95th percentile aviators were determined (Tables 3-5).

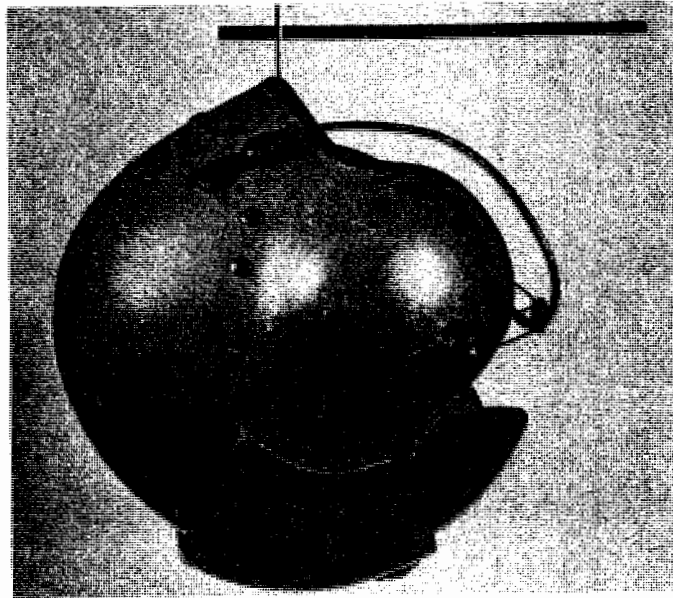
### RESULTS AND DISCUSSION

The idealized trapezoidal acceleration pulse applied vertically at the base of the spine is shown in Figure 13 along with an actual record of a MK-J5(D) acceleration time history. The trapezoidal acceleration pulse was used to study several configurations of the model as given in Table 6. The configurations were selected mainly on the basis of spinal alignment data reported by Kaplan (1972) for the face curtain (position 1) and secondary "D" ring (position 2) ejection positions of three aviators seated in the MK-J5(D) ejection seat. Three aviators, 5th, 40th and 95th percentile men in terms of their sitting height, were selected to represent their anthropometric class. The constraints were varied so that the effects of seat back, face curtain and shoulder harness restraints could be studied. Additionally, the lumbar spinal alignment induced by an improved McDonnell lumbar pad discussed by Sanford and Kellet (1966) was studied.

The first configuration served to define the basic unconstrained response of the spinal column to caudocephalad acceleration and was used as a baseline to observe changes induced by the addition of restraints. The graphical results shown in Figures 14 through 18 give the unconstrained response of the 5th percentile aviator. In these and all following figures, axial compressive forces, bending moments which induce compression in the anterior half of the vertebral body, and shearing forces directed anteriorly are plotted with positive ordinates. As could be expected of the case without restraint, the torso flexes rapidly and reaches a horizontal position at 170 ms. In order to study the regional variation in forces, an "effective" normal compressive stress was calculated according to the strength of materials formula:  $\sigma_c = P/A \pm Mc/I$ . Positive values of this function indicate the existence of net compressive stress on the anterior half of the vertebral body. Additionally, an effective axial stress,  $\sigma_A = P/A$ , was calculated. Both effective stress functions were calculated using the forces



(a)



(b)

Figure 12. Center of Gravity of Aviator's Helmet

TABLE 3  
5TH PERCENTILE ANTHROPOMETRIC DATA

VERTEBRAL LEVEL	DISC AREA (IN <sup>2</sup> )	DISC HEIGHT (IN)	AREA MOMENT OF INERTIA (IN <sup>4</sup> )	MASS (LB-SEC <sup>2</sup> /IN)	ROTATORY INERTIA (LB-SEC <sup>2</sup> -IN)	VERTEBRAL HEIGHT (IN)	ECCENTRICITY (IN)	POS 1 ANGLE (DEG)	POS 2 ANGLE (DEG)	MCDONNELL LUMBAR PAD ANGLE (DEG)
L5	2.72	0.36	0.306	0.0118	0.0528	1.32	0.89	-4.	-6.	23.
L4	2.66	0.48	0.220	0.0106	0.0481	0.98	1.06	-8.	-14.	24.
L3	2.44	0.42	0.282	0.0104	0.0472	1.29	1.19	-5.	-6.	22.
L2	2.22	0.41	0.169	0.0091	0.0442	1.12	1.11	-2.	-6.	21.
L1	1.94	0.38	0.135	0.0092	0.0518	1.02	1.17	2.	0.	19.
T12	1.97	0.28	0.119	0.0083	0.0490	1.03	1.37	7.	6.	17.
T11	1.84	0.17	0.115	0.0067	0.0383	1.13	1.36	7.	9.	15.
T10	1.52	0.17	0.102	0.0057	0.0326	1.15	1.44	18.	16.	13.
T9	1.47	0.15	0.097	0.0063	0.0365	0.85	1.51	17.	11.	11.
T8	1.36	0.15	0.080	0.0056	0.0339	0.85	1.26	8.	19.	8.
T7	1.32	0.15	0.065	0.0050	0.0320	0.76	1.08	23.	19.	16.
T61	1.30	0.14	0.060	0.00324	0.2246	5.16	1.10	23.	45.	23.
C74	1.20	0.24	0.046	0.0152	0.0564	3.11	0.00	23.	10.	23.
C31	1.12	0.24	0.038	0.0030	0.0064	1.26	0.00	20.	7.	20.
H	0.49	0.24	0.013	0.0426	0.5130	1.10	0.70	0.	0.	0.

TABLE 4

## 40TH PERCENTILE ANTHROPOMETRIC DATA

VERTEBRAL LEVEL	DISC AREA (IN <sup>2</sup> )	DISC HEIGHT (IN)	AREA MOMENT OF INERTIA (IN <sup>4</sup> )	MASS (LB-SEC <sup>2</sup> /IN)	ROTATORY INERTIA (LB-SEC <sup>2</sup> -IN)	VERTEBRAL HEIGHT (IN)	ECCENTRICITY (IN)	POS 1 ANGLE (DEG)
L5	2.72	0.36	0.306	0.0132	0.0720	1.32	0.33	-1.
L4	2.66	0.48	0.220	0.0125	0.0698	1.38	0.59	-6.
L3	2.44	0.42	0.282	0.0121	0.0689	1.29	1.06	0.
L2	2.22	0.41	0.169	0.0110	0.0641	1.12	0.98	-3.
L1	1.94	0.38	0.135	0.0107	0.0669	1.22	1.04	-3.
T12	1.97	0.28	0.119	0.0093	0.0599	1.33	1.20	-11.
T11	1.84	0.17	0.115	0.0086	0.0574	0.83	1.21	-10.
T10	1.52	0.17	0.102	0.0071	0.0484	1.15	1.38	0.
T9	1.47	0.15	0.097	0.0077	0.0522	1.10	1.44	10.
T8	1.36	0.15	0.080	0.0072	0.0489	0.95	1.13	9.
T7	1.32	0.15	0.065	0.0071	0.0515	0.76	1.01	6.
T6	1.30	0.14	0.060	0.0359	0.2558	4.51	1.05	27.
C7	1.20	0.24	0.046	0.0152	0.0553	2.86	0.00	21.
C3	1.12	0.24	0.038	0.0030	0.0063	0.96	0.00	11.
H	0.49	0.24	0.013	0.0426	0.5130	1.10	0.70	0.

TABLE 5  
95TH PERCENTILE ANTHROPOMETRIC DATA

VERTEBRAL LEVEL	DISC AREA (IN <sup>2</sup> )	DISC HEIGHT (IN)	AREA MOMENT OF INERTIA (IN <sup>4</sup> )	MASS (LB-SEC <sup>2</sup> /IN)	ROTATORY INERTIA (LB-SEC <sup>2</sup> -IN)	VERTEBRAL HEIGHT (IN)	ECCENTRICITY (IN)	POS 1 ANGLE (DEG)
L5	2.72	0.36	0.306	0.0152	0.0879	1.32	0.72	11.
L4	2.66	0.48	0.220	0.0153	0.0878	1.38	0.92	-1.
L3	2.44	0.42	0.282	0.0146	0.0870	1.39	1.15	-3.
L2	2.22	0.41	0.169	0.0138	0.0807	1.32	1.07	-13.
L1	1.94	0.38	0.135	0.0130	0.0795	1.42	1.13	-3.
T12	1.97	0.28	0.119	0.0109	0.0691	1.43	1.32	-11.
T11	1.84	0.17	0.115	0.0115	0.0733	1.08	1.31	-18.
T10	1.52	0.17	0.102	0.0092	0.0615	1.15	1.42	-15.
T9	1.47	0.15	0.097	0.0098	0.0652	0.95	1.49	-10.
T8	1.36	0.15	0.080	0.0096	0.0615	0.95	1.22	0.
T7	1.32	0.15	0.065	0.0103	0.0678	0.96	1.05	5.
T61	1.30	0.14	0.060	0.0412	0.3519	5.26	1.09	5.
C74	1.20	0.24	0.046	0.0152	0.0577	3.01	0.00	19.
C31	1.12	0.24	0.038	0.0030	0.0064	1.16	0.00	-2.
H	0.49	0.24	0.013	0.0426	0.5130	1.10	0.70	0.

20

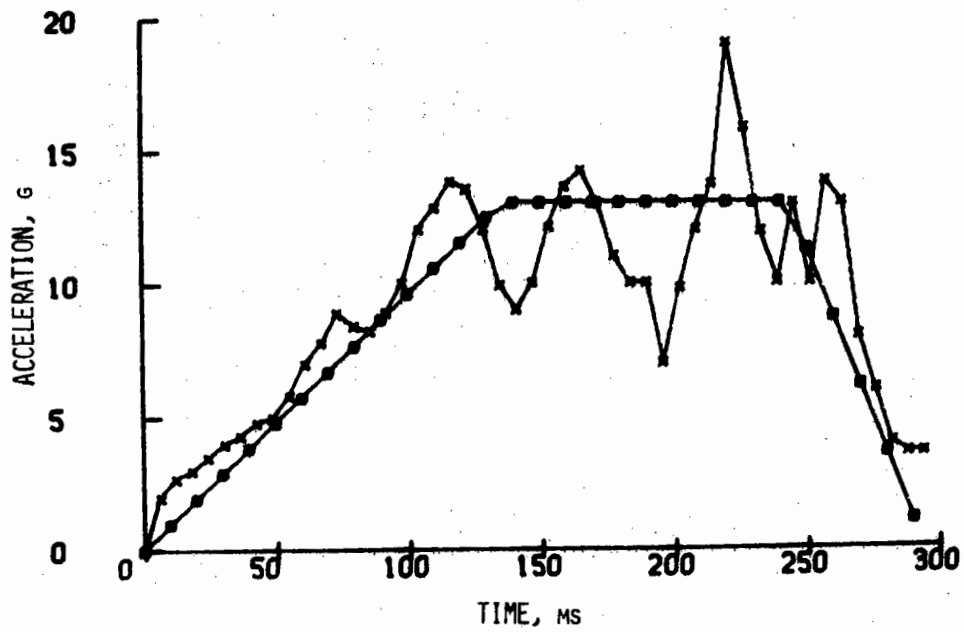


Figure 13. MK-J5(D) Acceleration Pulse with Trapezoidal Idealization

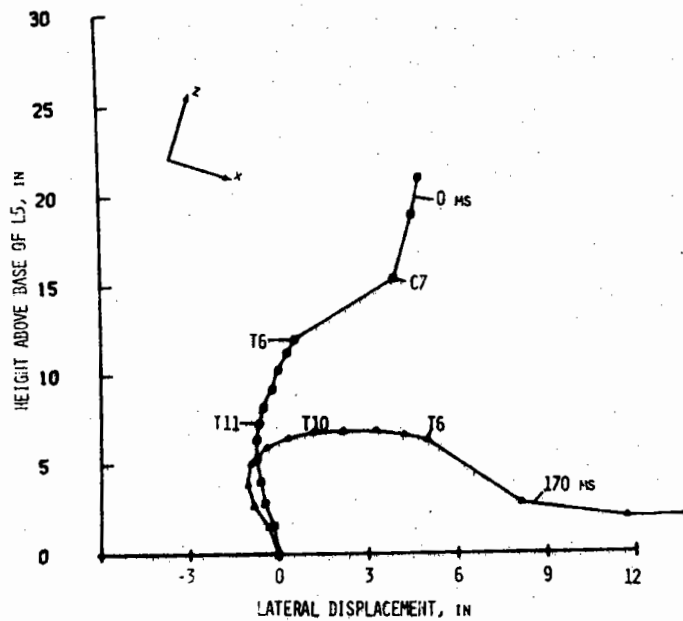


Figure 14. Spinal Alignment, 5th Percentile, Position 1, Unrestrained

TABLE 6  
MODEL CONFIGURATIONS

<u>CONFIGURATION</u>	<u>PERCENTILE MAN (Sitting Height)</u>	<u>INITIAL SPINAL POSITION</u>	<u>RESTRAINTS</u>
1	5	1	None
2(a)	5	1	Face Curtain, Shoulder Harness
2(b)	40	1	Face Curtain, Shoulder Harness
2(c)	95	1	Face Curtain, Shoulder Harness
3(a)	5	1	Face Curtain, Shoulder Harness, Seat Back
3(b)	40	1	Face Curtain, Shoulder Harness, Seat Back
3(c)	95	1	Face Curtain, Shoulder Harness, Seat Back
4	5	2	Shoulder Harness, Seat Back
5	5	McDonnell Pad	Face Curtain, Shoulder Harness, Seat Back

and moments existing on the superior surface of the rigid vertebral body. Figure 15 shows  $\sigma_c$  for the unconstrained 5th percentile aviator. The maximum normal stress is seen to occur at L5 but this peak is due to the clamped beam boundary condition. Thus the secondary peak at L2 is more indicative of the location of maximum stress. Figure 16 shows the variation of maximum axial force and effective axial stress for the unconstrained case. The maximum axial force is found at the base of the spine but the maximum axial stress occurs in the lower and middle thoracic region. This was found to be true for all cases studied. In several instances (Table 7), maximum axial stresses did occur in the upper lumbar region but when this was the case secondary maximums, usually only several percent less in magnitude, were found higher in the column. The axial stress was relatively constant along the column. It appears that the variation of cross-sectional area of the discs and vertebrae is such that a constant axial stress is maintained in the column. The time histories of the axial force, bending moment, and shear force on the superior surface of L1 are shown in Figure 17. The time of maximum normal stress corresponds to the occurrence of peak bending moment since the axial force is relatively constant. Figure 18 shows the axial force and bending moment distribution along the spinal column at 170 ms.

Results for Configuration 2 are given in Figures 19 through 23. Figure 19 shows the displacements of the spinal column when the lower vertebrae are not constrained. Comparing Figures 14 and 19, we see that the shoulder harness and face curtain prevent flexion of the torso. Thus, the resulting deformation of the column is restricted mainly to the lower thoracic and lumbar regions. This serves to place the maximum normal stress at points of maximum spinal curvature as can be seen from Figure 20. It should be emphasized at this point that the displacement curve is the loci of all the midpoints of the inferior vertebral endplates while the forces are taken with respect to the superior endplates. The 5th percentile aviator has a maximum normal stress at L1, the 40th at T12, and the 95th at T9. These dynamic stress levels coincide almost exactly with the static observations of Kaplan (1972) who predicted that maximum stress levels would occur at T12, T11, and T9, respectively. Thus, the curvatures as determined from spinal alignment x-rays under static conditions are useful for determining spinal injury levels for this ejection configuration. Later results indicate the same to be true for all configurations utilizing the face curtain mode of egress. For the head free or secondary "D" ring configuration, position 2, the maximum normal stress occurs in the middle and upper thoracic region due to the effects of head movement and head impact on the anterior chest wall. Figure 21 shows the maximum axial force and bending moment distribution for the 5th percentile aviator. The bending moment values are zero for L5 and L4 since only moments tending to flex the column were considered. The time histories of axial force, bending moment, and shearing force for L1, the level of maximum normal stress for the 5th percentile aviator, are given in Figure 22. As can be seen, the axial force level parallels the rise of the acceleration as given in Figure 13. Since the axial force remains relatively constant after 130 ms, the bending moment dictates where the maximum normal stress occurs. The head restraint

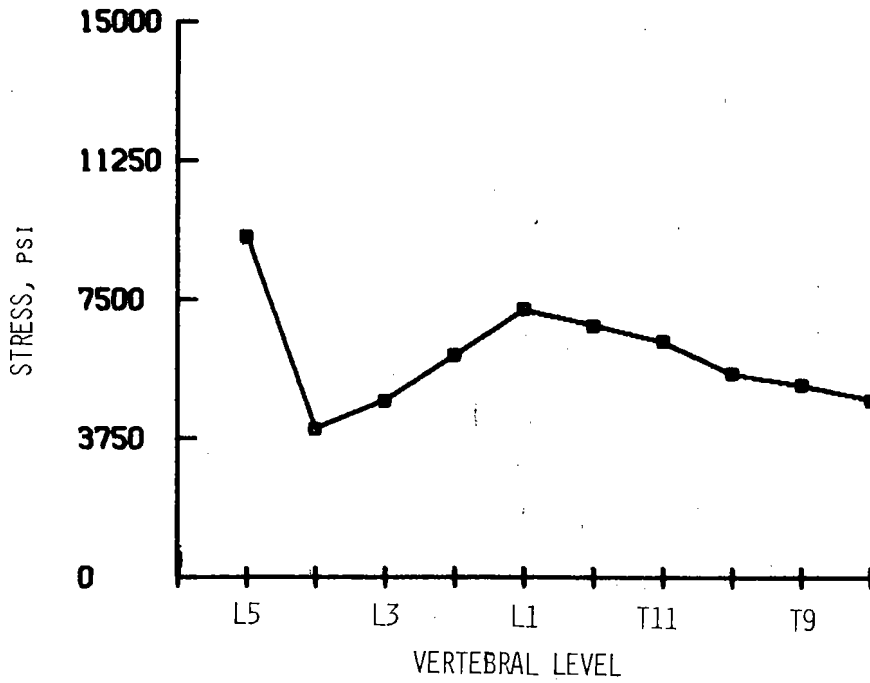


Figure 15. Maximum Normal Stress, 5th Percentile, Position 1, Unrestrained

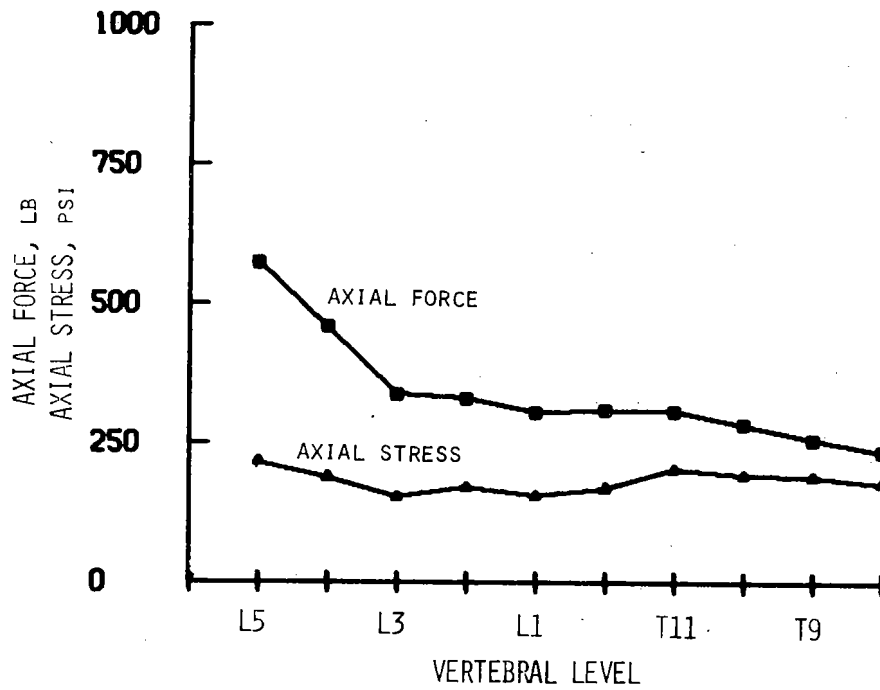


Figure 16. Maximum Axial Forces and Stresses, 5th Percentile, Position 1, Unrestrained

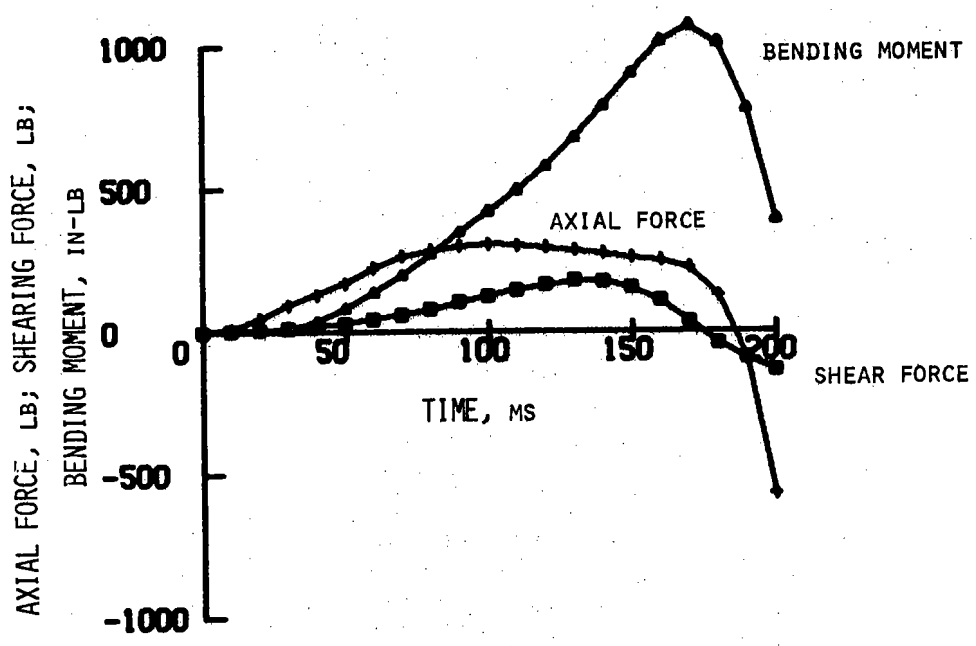


Figure 17. Time History of Axial Force, Shear Force, and Bending Moment on Superior Surface L1, 5th Percentile, Position 1, Unrestrained

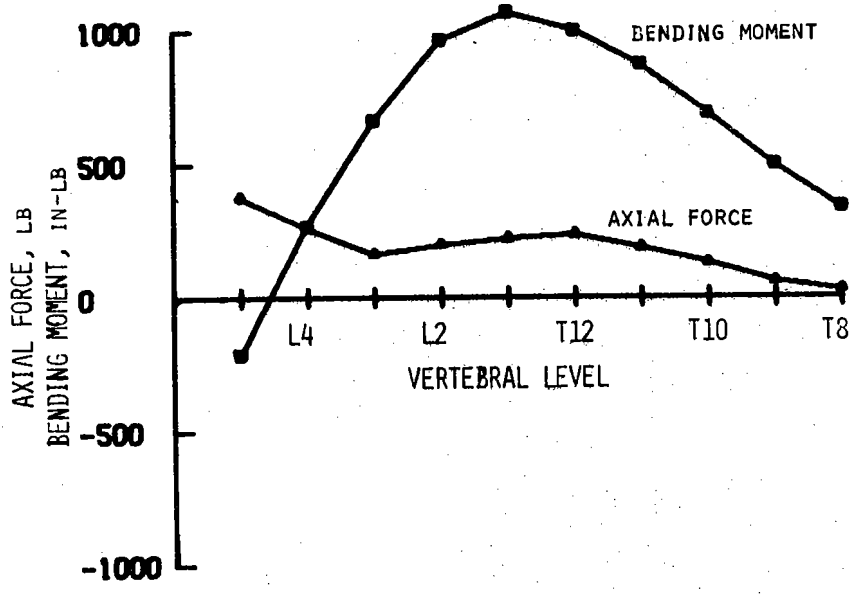


Figure 18. Axial Force and Bending Moment Distribution at 170 ms, 5th Percentile, Position 1, Unrestrained

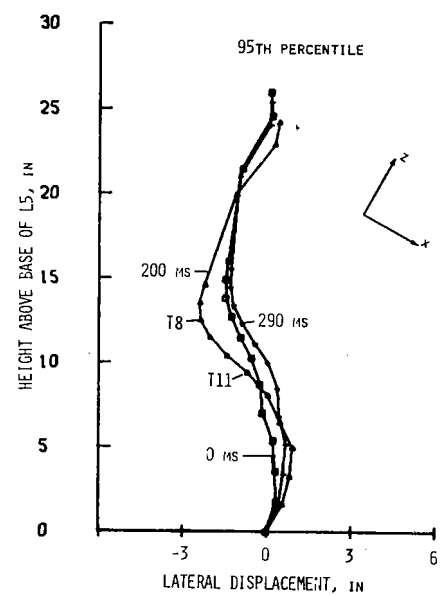
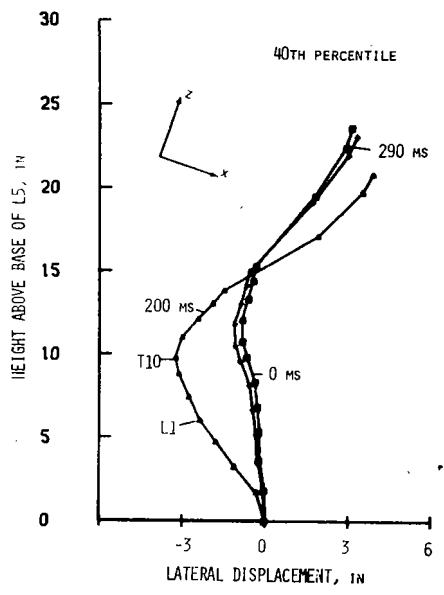
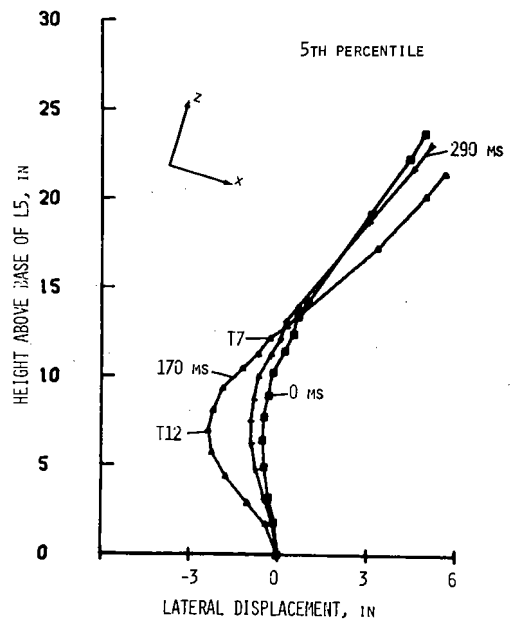


Figure 19. Spinal Alignment, 5th, 40th, 95th Percentile, Position 1, Face Curtain, Shoulder Harness

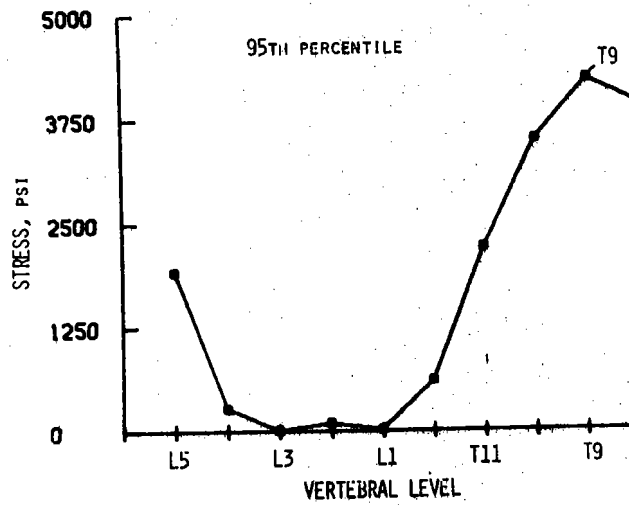
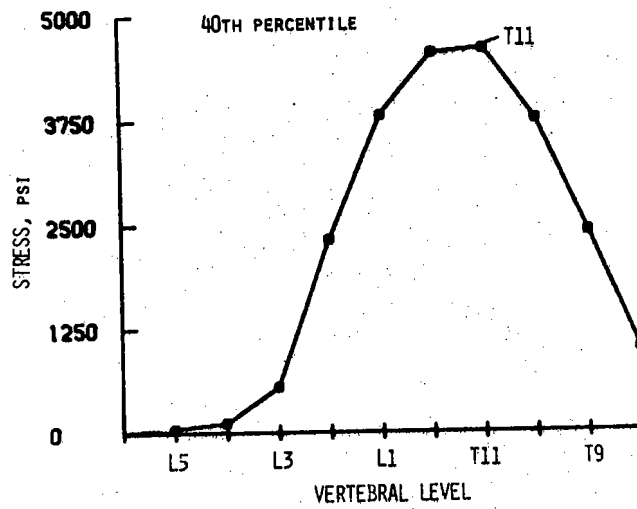
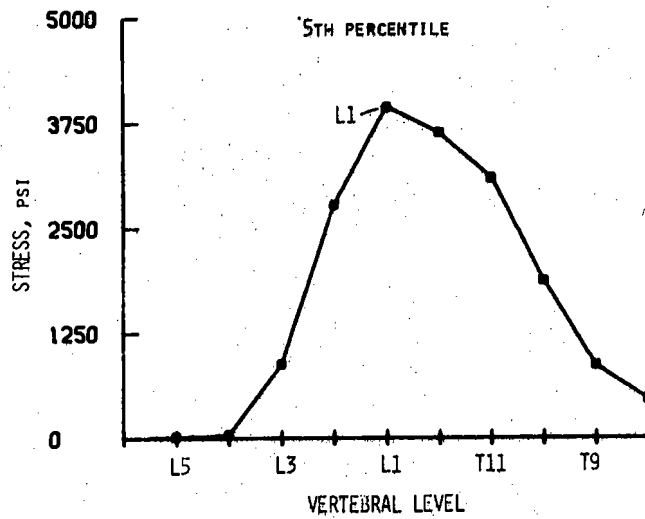


Figure 20. Maximum Normal Stress, 5th, 40th, 95th Percentile, Position 1, Face Curtain, Shoulder Harness

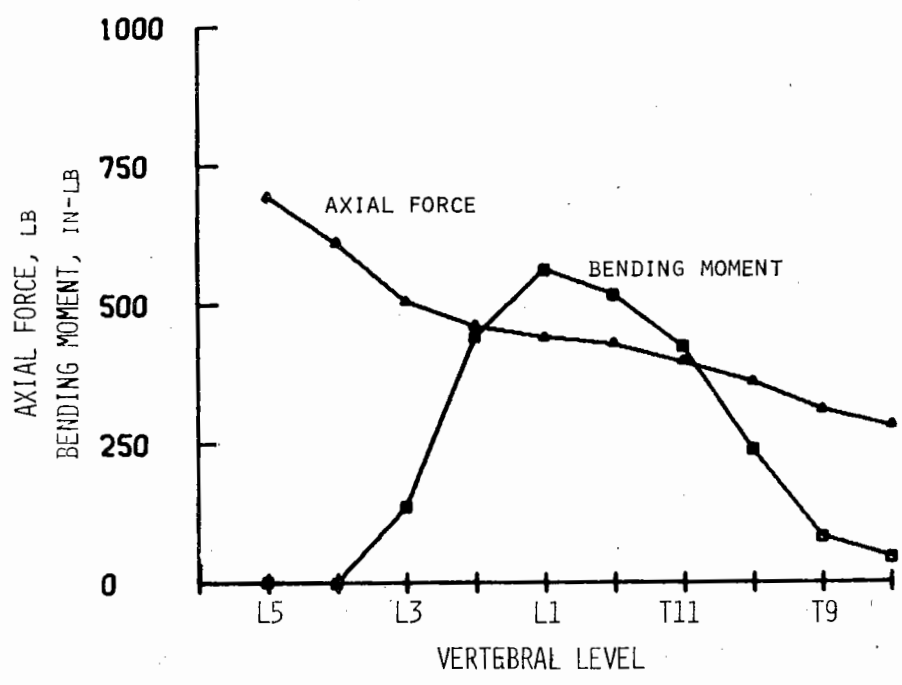


Figure 21. Maximum Axial Force and Bending Moment Distribution, 5th Percentile, Position 1, Face Curtain, Shoulder Harness

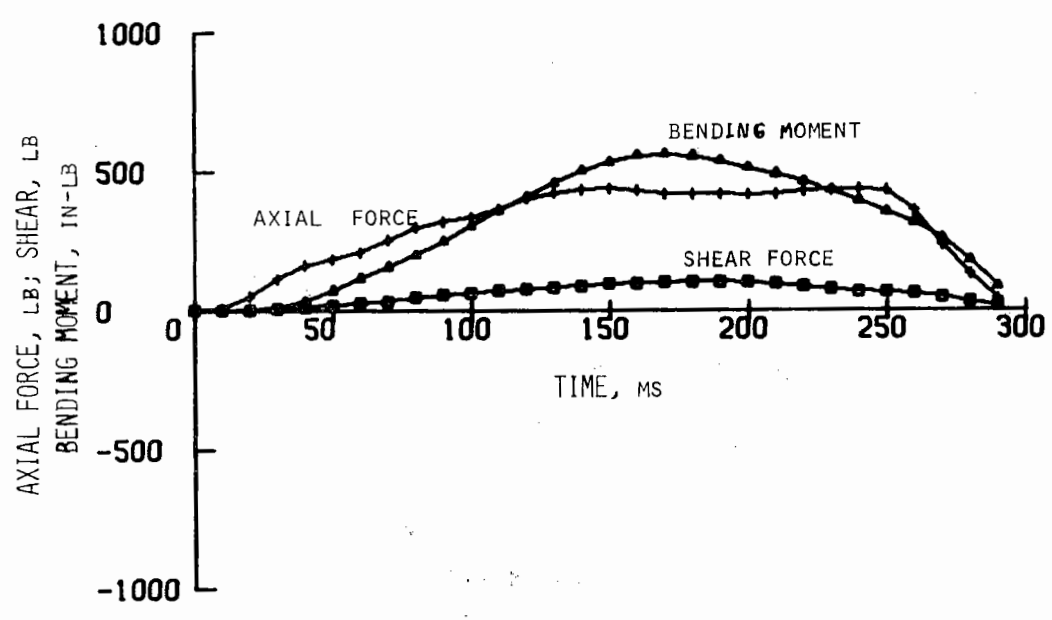


Figure 22. Time History of Axial Force, Shear Force, and Bending Moment of Superior Surface of L1, 5th Percentile, Position 1, Face Curtain, Shoulder Harness

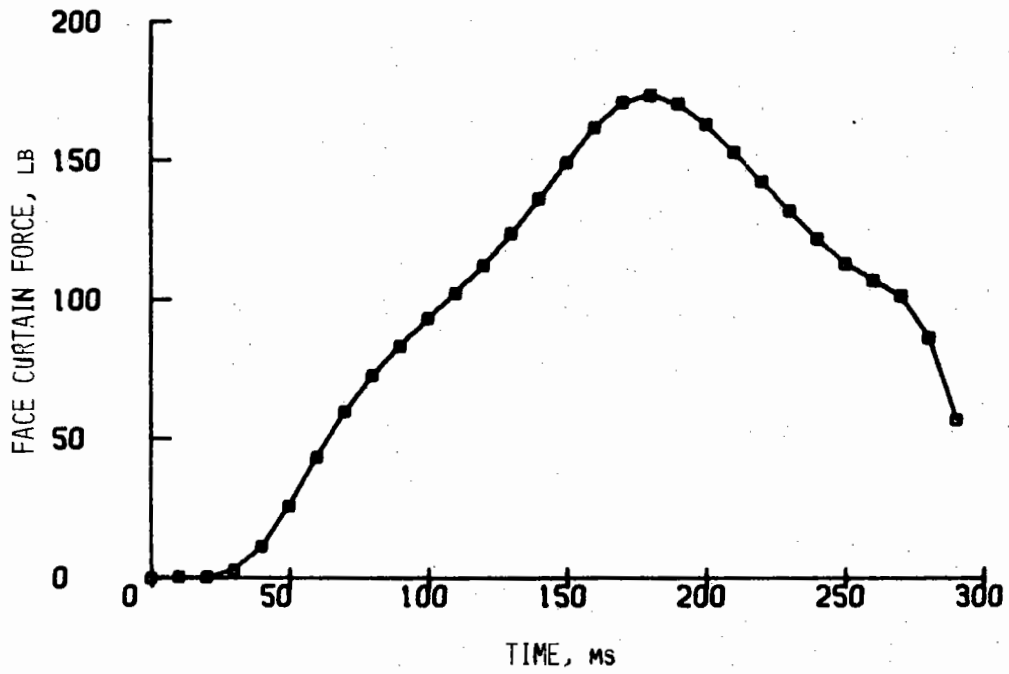


Figure 23. Face Curtain Force, 5th Percentile, Position 1, Face Curtain, Shoulder Harness

force is shown in Figure 23. Peak values of this force are in the same order of magnitude as the results of Vulcan and King (1970).

The results of Configuration 3, shown in Figures 24 through 27, give the outputs for the 5th, 40th and 95th percentile aviator with face curtain, shoulder harness and seat back constraints. The seat back constraint was idealized to give lateral but no vertical support. There probably exists a certain amount of vertical support due to friction, as is the case with the shoulder harness, but this effect was neglected. Comparing the results of Figures 19 and 24 shows that the lateral restraint prevents the bowing of the lower column. Figure 25 shows a 75% reduction in normal stress due to the lateral restraint. The amplitudes of peak normal stress have also generally shifted to a level lower in the spinal column. The 5th percentile peak occurs at L2, the 40th at T10, and the 95th at T10. When lateral movement is curtailed, the greater influence of axial stress on the normal stress is apparent. The axial stress comprises approximately 30% of the normal stress with lateral support whereas with no lateral support, it only represented 8%. Hence, one can conclude that lateral support, in the form of a properly designed back pad and harness system, can prevent excessive anterior compressive stresses with its resulting anterior lip fracture. The seat back itself would not necessarily provide the degree of support required. There is probably a substantial degree of movement allowed since the curvatures of the spine would prevent intimate contact. Additionally, the rib cage humps posteriorly and prevents spinous processes from contacting the seat back. Since a lateral deflection of only 0.5 in. is sufficient to cause large bending stresses, a pad which is specifically and intimately contoured for each aviator might be one of the simpler solutions to the ejection problem. Alternatively, the support might be designed to place all spinal regions in extension so as to load the posterior lamina and pedicles and thereby increase the effectively loaded area. Figure 26 shows the maximum axial force and axial stress levels. Again, it can be seen that axial stress levels remain fairly constant. The increase in axial force levels from the 5th to 95th percentile aviators is due to the increase in mass. However, it should be noted that the cross-sectional area of the discs and vertebrae used were the same for all runs. Since disc and vertebral areas increase in proportion to overall body size, it is possible that the spines of each aviator would be subjected to the same axial stress levels. Thus, the initial spinal configuration, through its influence on the location of maximum bending stress, would govern the level of anterior spinal fracture. The time histories of force, bending moment, and shearing force at L2 for the 5th percentile aviator are given in Figure 27.

Figures 28 through 31 give the results of Configuration 4, i.e., the 5th percentile with shoulder harness and seat back restraint, but the head is free. The displacement of the T1-6 segment seen in Figure 28 would not be as pronounced if the column had been discretized. If this had been done, the bending and axial forces would have been distributed over the additional discs and vertebrae. However, the

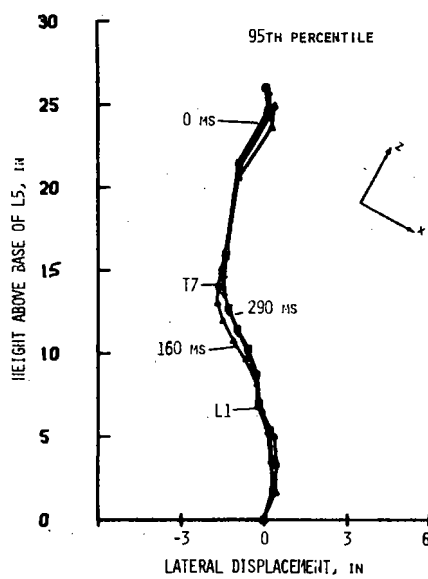
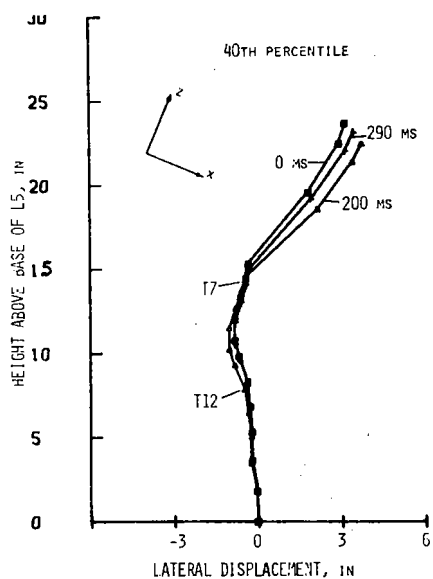
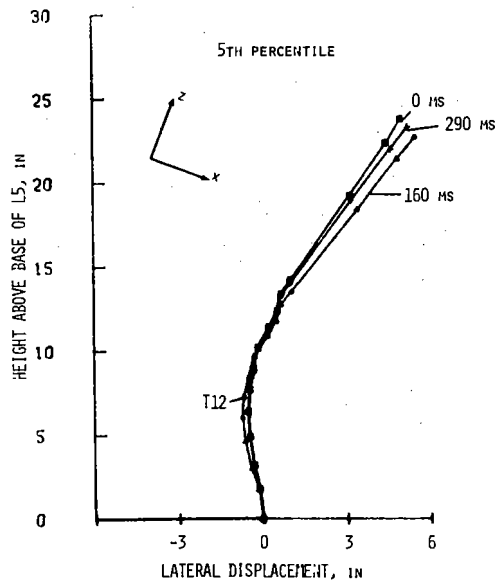


Figure 24. Spinal Alignment, 5th, 40th, 95th Percentile, Position 1, Face Curtain, Shoulder Harness, Seat Back

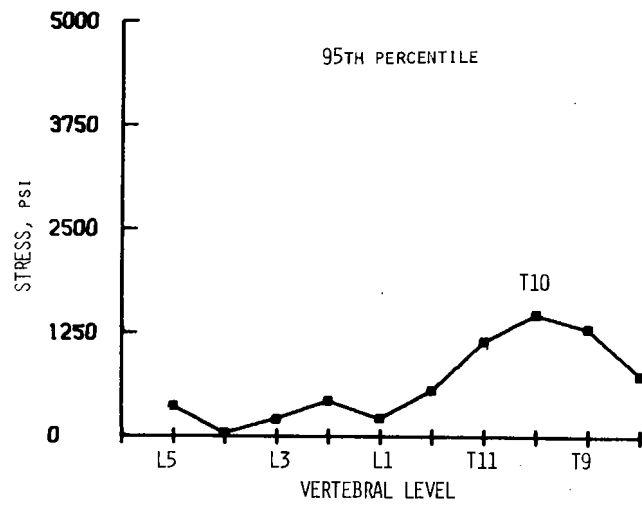
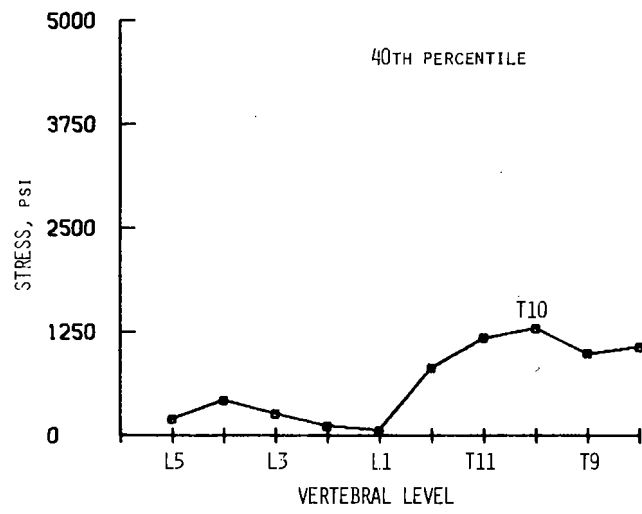
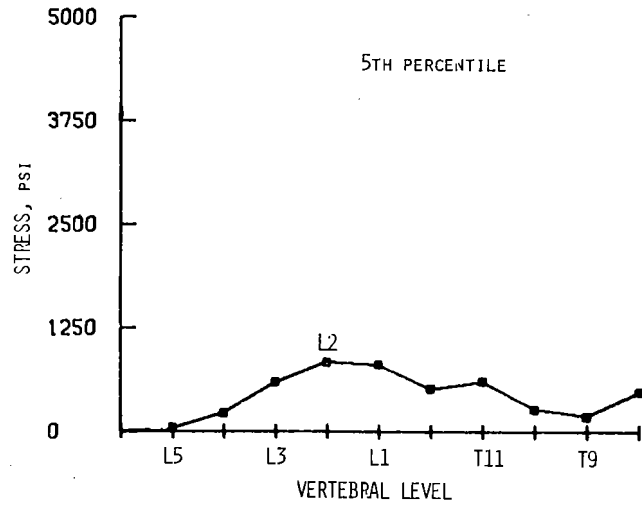


Figure 25. Maximum Normal Stress, 5th, 40th, 95th Percentile, Position 1, Face Curtain, Shoulder Harness, Seat Back

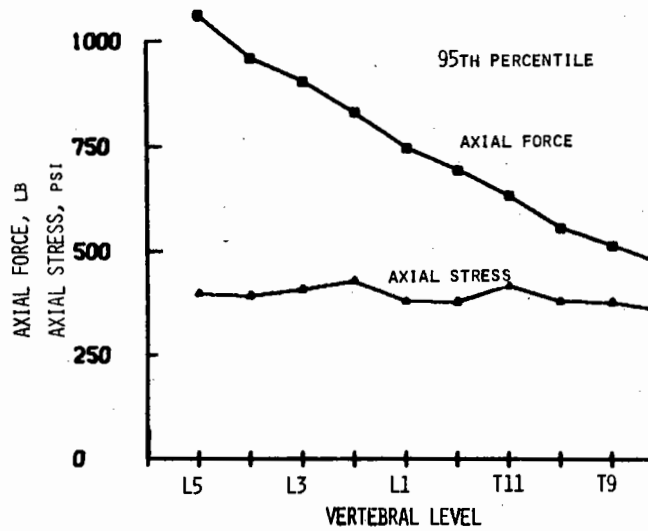
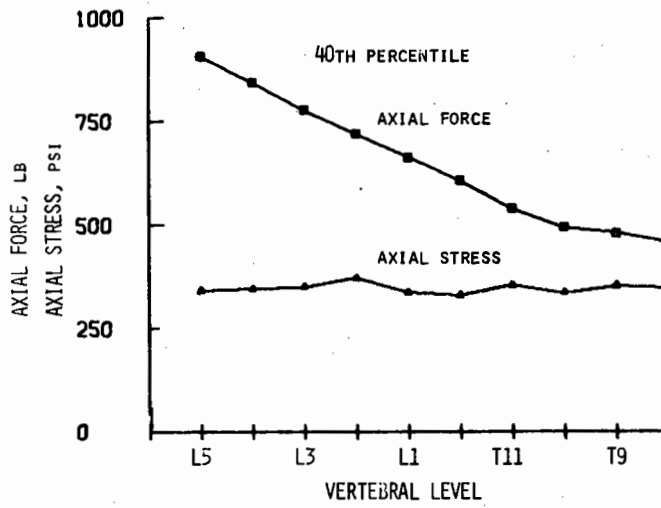
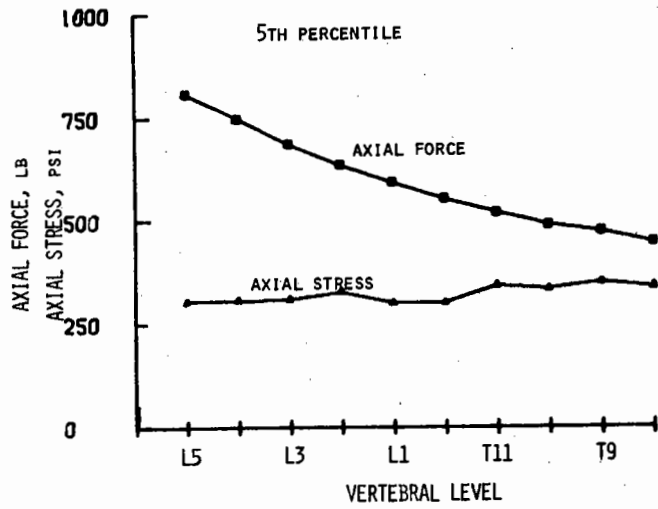


Figure 26. Maximum Axial Forces & Stresses, 5th, 40th, 95th Percentile, Position 1, Face Curtain, Shoulder Harness, Seat Back

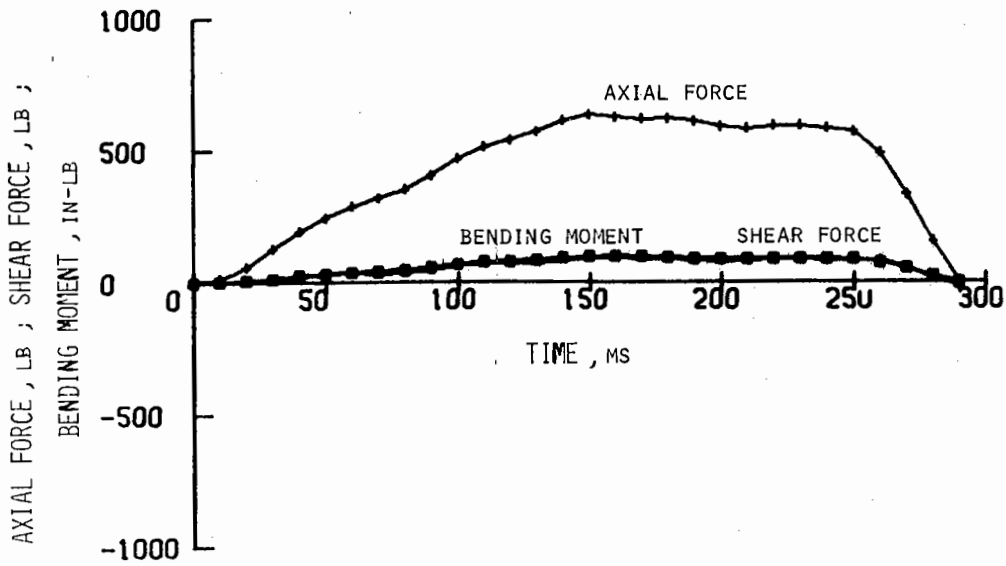


Figure 27. Time History of Axial Force, Shearing Force and Bending Moment on Superior Surface of L2, 5th Percentile, Position 1, Face Curtain, Shoulder Harness, Seat Back

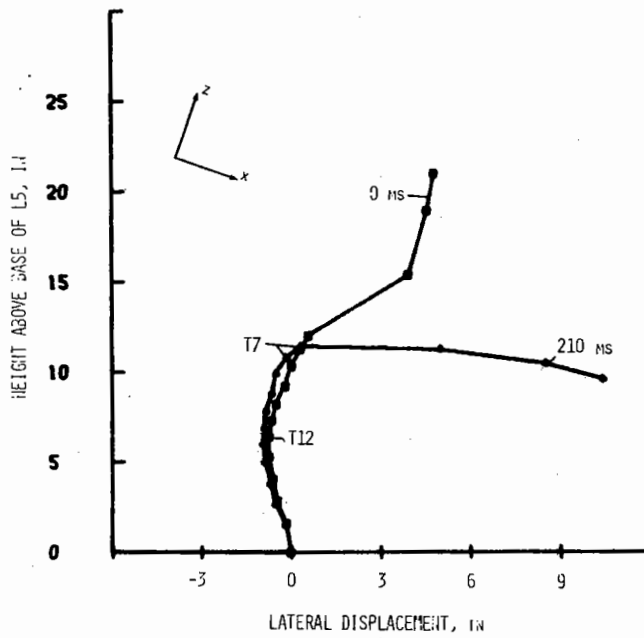


Figure 28. Spinal Alignment, 5th Percentile, Position 2, Shoulder Harness, Seat-Back

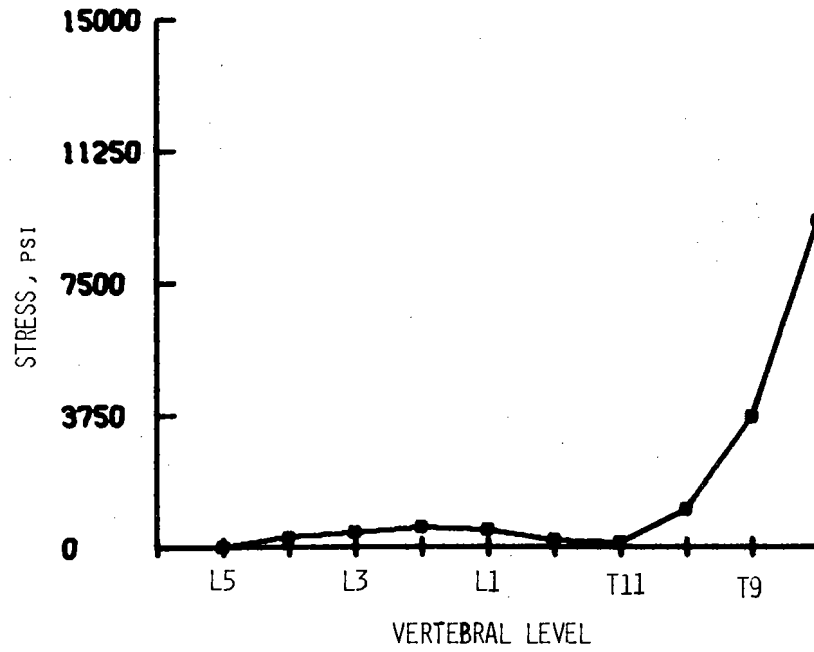


Figure 29. Maximum Normal Stress, 5th Percentile, Position 2, Shoulder Harness, Seat Back

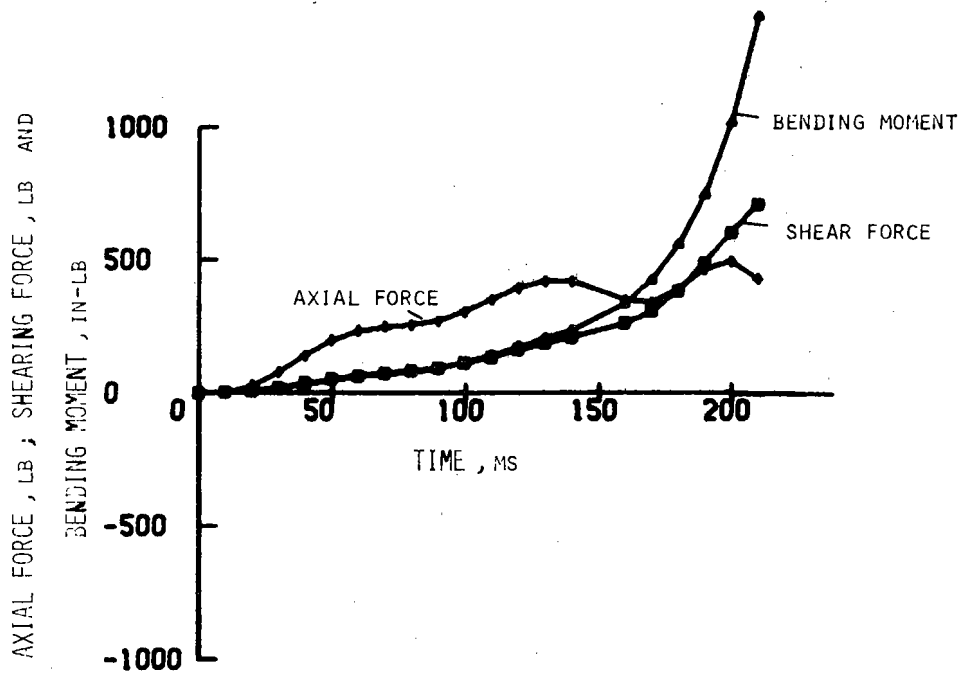


Figure 30. Time History of Axial Force, Shearing Force, and Bending Moment on Superior Surface of T7, 5th Percentile, Position 2, Shoulder Harness, Seat Back

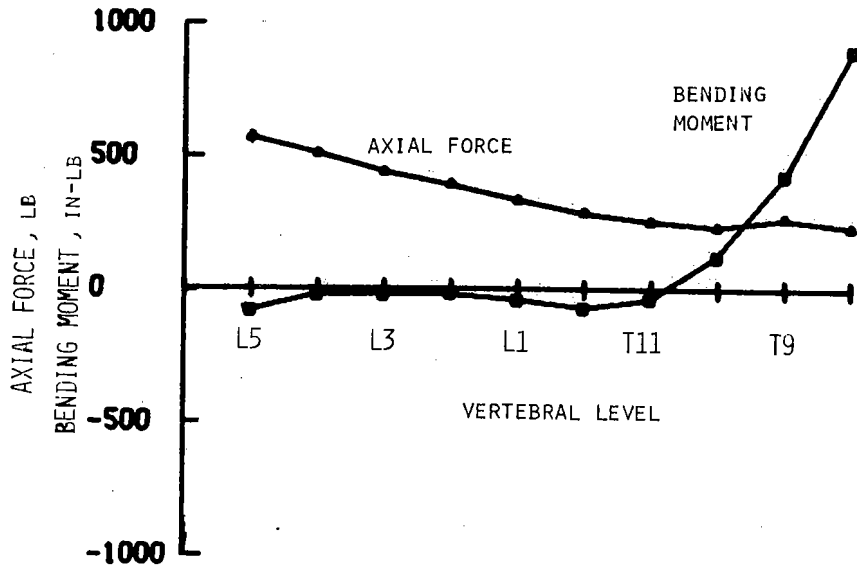


Figure 31. Maximum Axial Force and Bending Moment, 5th Percentile, Position 2, Shoulder Harness, Seat Back

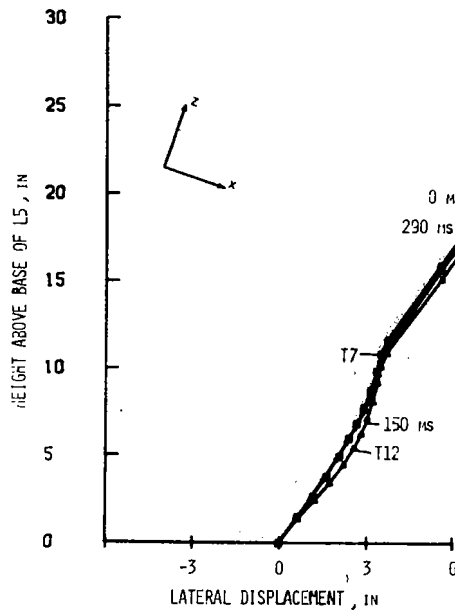


Figure 32. Spinal Alignment, 5th Percentile, McDonnell Lumbar Pad, Face Curtain, Shoulder Harness, Seat Back

configuration does serve to show that the maximum normal stress is shifted to the upper thoracic region (Figure 29) when the face curtain is not used. It also explains the observation of Latham (1957) that inadvertent ejection with loose harness and failure to utilize the face curtain always resulted in a fracture in the region of T6. The time histories of axial force, bending moment, and shearing force at T7 are given in Figure 30. Figure 31 gives the maximum axial force and bending moment distribution for the spinal column with the head free. In each figure the effect of the freely displacing head can be seen.

One final configuration was studied. Sanford and Kellet (1966) reported on an improved lumbar pad to be used by the U.S. Navy in the MK-H5/H7F-1 seat. The lumbar curvatures reported for a 15th percentile aviator were used along with the anthropomorphic data for the 5th percentile aviator as reported by Kaplan (1972). Figures 32 through 35 give the results for the face curtain, shoulder harness and seat restraint configuration. The main effect of the lumbar pad is to place the column in hyperextension as can be seen in Figure 32. This allows the posterior vertebral elements to carry a portion of the axial and bending load and thus greatly decreases the anterior stress as can be seen in Figure 33. However, the axial force levels and stresses are increased. Figure 34 shows the time history of the axial force, bending moment and shearing stress at T7. Figure 35 gives the axial force and bending moment distribution at 150 ms.

A synopsis of the results for the various runs is given in Table 7. Maximum axial forces are seen to occur in the lower lumbar region. However, since disc cross-sectional areas vary, the maximum axial stresses occur in the lower thoracic and upper lumbar regions. Thus, initial configurations which place the level of maximum bending stress in the thoracolumbar region should be avoided, since the maximum normal stress then indicates a strong probability of anterior lip fracture there. Yamada (1970) found compressive vertebral failure occurred when the body of the vertebra was exposed to stresses greater than 908 to 1249 lb/in<sup>2</sup>. Values in Table 7 indicate that with inadequate lateral support stress levels of up to 200 to 300% of the failure level can occur. If the head is free, the stress levels obtained indicate a very strong likelihood of fracture. If one accepts the use of effective normal stress as a criterion, the necessity of utilizing the face curtain and having adequate seat back support is very clearly indicated.

The fact that the situation is not quite as critical as indicated in the preceding paragraph is probably due to two sources:

1. One of the basic assumptions of the Orne-Liu model is the idealization of the soft tissues as a rigid body. Thus, of the two assigned properties of the soft tissues, inertia and elasticity, only the inertia has been retained. This is a cautious formulation of the problem since the deformations of the soft tissues would alleviate to a certain extent, the stresses experienced by the vertebrae. This approach was adopted to make the analytic problem tractable while

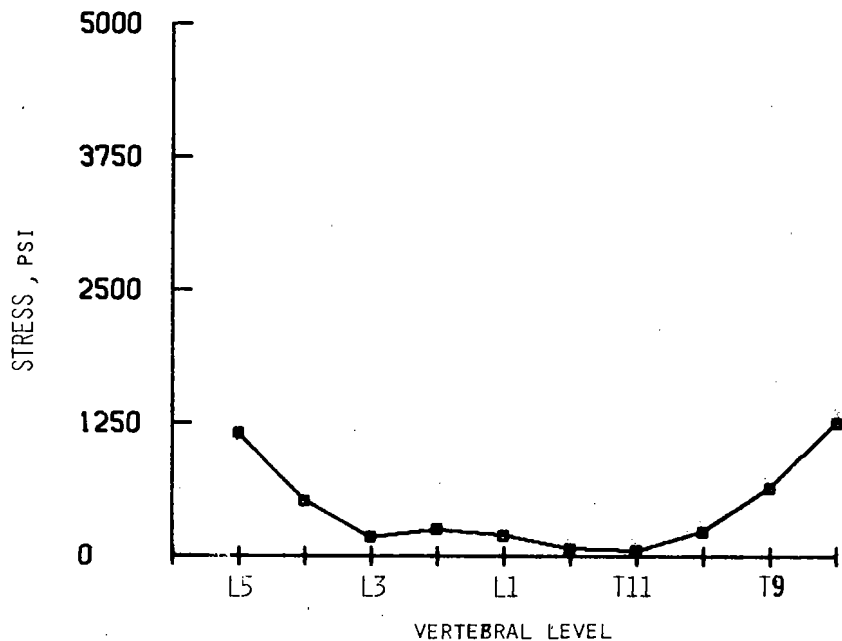


Figure 33. Maximum Normal Stress, 5th Percentile, Position 1, Face Curtain, Shoulder Harness, Seat Back, McDonnell Lumbar Pad

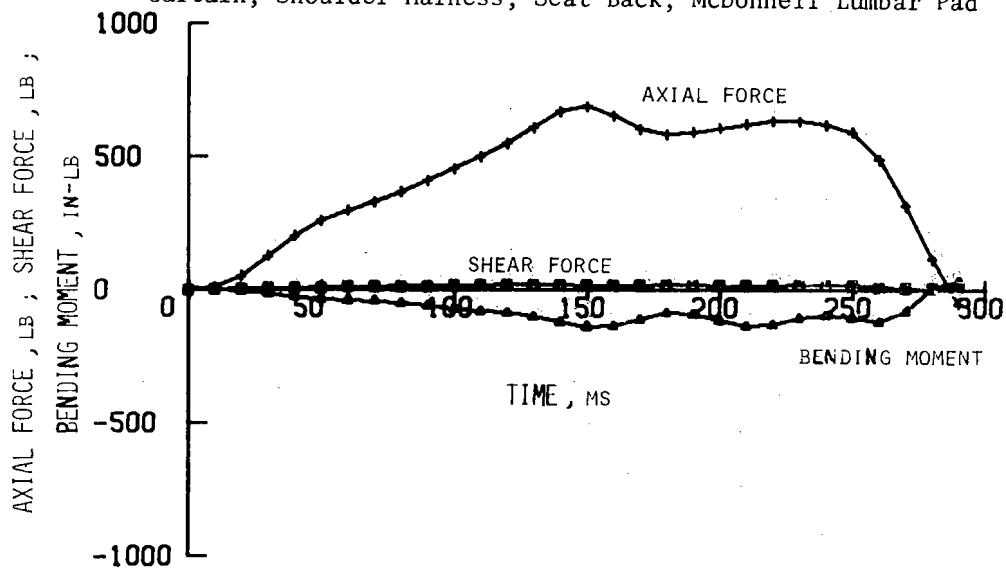


Figure 34. Time History of Axial Force, Shearing Force, and Bending Moment on Superior Surface of T7, 5th Percentile, Position 1, Face Curtain, Shoulder Harness, Seat Back, McDonnell Lumbar Pad

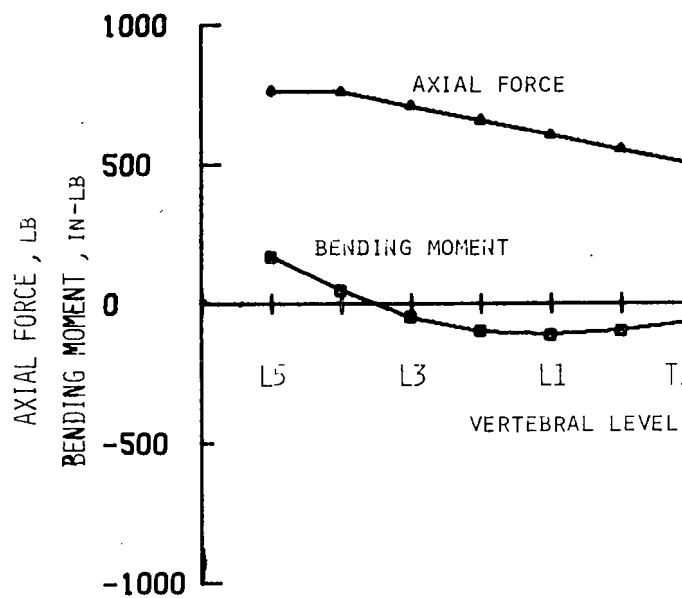


Figure 35. Axial Forces and Bending Moments at T = 150 ms, 5th Percentile, Position 1, Face Curtain, Shoulder Harness, Seat Back, McDonnell Lumbar Pad

TABLE 7  
TEST RESULTS

CONFIGURATION	PERCENTILE AVIATOR	MAXIMUM AXIAL FORCE			MAXIMUM AXIAL STRESS			MAXIMUM BENDING MOMENT†			MAXIMUM NORMAL STRESS		
		lb	VERT. LEVEL	TIME ms	psi	VERT. LEVEL	TIME ms	psi	VERT. LEVEL	TIME ms	psi	VERT. LEVEL	TIME ms
Unrestrained	5	457	L5	130	301	T11	150	1065*	L1	170	7211	L1	170
FC, SH	5	610	L5	150	260	T11	150	561	L1	170	3946	L1	170
	40	698	L5	150	282	L2	150	653	T12	200	4555	T12	200
	95	878	L5	150	402	L2	150	477	T9	180	4239	T9	180
FC, SH, SB	5	746	L5	150	346	T9	160	91	L2	160	832	L2	160
	40	840	L5	160	369	L2	160	136	T10	170	1286	T10	170
	95	959	L5	140	428	L2	140	158	T10	160	1463	T10	160
Head Free, SH, SB	5	711	L5	140	156	T9	130	1416	T7	210	15713	T7	210
FC, SH, SB, MLP	5	859	L5	150	349	T11	150	98*	T7	150	1365	T7	150

FC = Face Curtain

SH = Shoulder Harness

SB = Seat Back

MLP = McDonnell Lumbar Pad

† in-lb

• Secondary Maximum chosen since L5 was clamped.

providing an upper bound estimate of the force levels found in the real case.

2. The failure loads given by Yamada (1970) are from quasistatic tests. It is well-known that at the high strain rate encountered in pilot ejection, the fracture stress is considerably higher than indicated by these values.

#### CONCLUSIONS

1. Spinal alignment prior to ejection, i.e., initial configuration, is a major factor in determining the location and magnitude of maximum vertebral stresses for a given set of restraints.
2. A properly designed back pad and harness system could prevent excessive anterior vertebral stresses when the face curtain is utilized.
3. The secondary "D" ring ejection position causes excessive normal stresses on the anterior edges of upper and middle thoracic vertebrae.
4. The face curtain and shoulder harness restraints serve to place the maximum normal stress in regions of maximum spinal curvature.
5. The locations of maximum normal stress levels can be predicted from spinal curvatures as determined from x-rays under static conditions for the face curtain ejection position.
6. The occurrence of maximum normal stress corresponds to the occurrence of maximum bending moments.
7. The effect of seat back restraint is to reduce maximum normal stresses and shift their location caudally.
8. A strong probability of anterior lip failure exists when the face curtain is not utilized or if inadequate (posterior-anterior) support is given to the spinal column.
9. The use of a lumbar pad which places the lumbar spine in extension greatly reduces the anterior normal stresses.
10. Maximum axial stresses occur in the lower thoracic and upper lumbar regions. Secondary maximums occur in the middle and upper thoracic column.
11. Variations in the cross-sectional areas of the discs and vertebrae result in a state of relatively constant axial stress being maintained in the spinal column during ejection.

## RECOMMENDATIONS

1. Any ejection seat design or improvements should be studied in a mathematical model such as used here to evaluate the effectiveness of the design or improvement in reducing the intervertebral joint stresses.
2. An experimental program is urgently needed to determine the stress levels required and the mechanisms involved in vertebral failure under combined states of stress. Proper design of restraint and support systems should be predicated on this knowledge.
3. Studies should be undertaken to provide a statistically significant set of spinal alignment data for pilots with a view toward developing a percentile spinal configuration population. To complement this data, anthropometric measurements needed for inertial properties determination should be gathered concurrently, i.e., height, weight, sitting height, chest depth, chest breadth, and hip breadth.
4. Upon completion of the experimental program, a spinal support system should be designed to minimize stresses during ejection. This should be accomplished using data gathered during the experimental phases and available mathematical modelling techniques.
5. Any improved restraint design should be capable of being installed on existing ejection seats.
6. Complete spinal alignment x-rays should be taken while the McDonnell lumbar pad and any other similar devices are in place. The data should then be subjected to analysis by currently available techniques.

#### REFERENCES

1. Bosee, R. A. and Payne, C. F., Jr., (1961), "The Mechanism and Cause of Vertebral Injuries Sustained on Ejection from U. S. Naval Aircraft." Air Crew Equipment Laboratory, Naval Air Material Center, Philadelphia, PA., Report #NAML-ACEL-467.
2. Ewing, C. L., (1971), "Non-Fatal Ejection Vertebral Fracture, U. S. Navy, Fiscal Years 1959 through 1965: Costs," Aerospace Med. 42(11):1226-1228.
3. Kaplan, B. H., (1972), "Evaluation of the Grumman MK-J5D Ejection Seat in Respect to Spinal Alignment," U. S. Army Aeromedical Research Laboratory, Report No. 72-10.
4. Latham, F., (1957), "A Study of Body Ballistics: Seat Ejections," Proc. Royal Society, B-147, pp. 121-139.
5. Liu, Y. K., Laborde, M. J. and Van Buskirk, W. C., (1971), "Inertial Properties of a Segmented Cadaver Trunk: Their Implications in Acceleration Injuries," Aerospace Med. 42(6):650-657.
6. Liu, Y. K. and Wickstrom, J. K., (1972), "Estimation of the Inertial Property Distribution of the Human Torso from Segmented Cadaveric Data," Proc. of the Symp. Perspectives in Biomedical Engineering, R. M. Kenedi, (Ed.), Glasgow, Scotland.
7. Moffatt, C. A. and Howard, R. H., (1968), "The Investigation of Vertebral Injury Sustained During Aircrew Ejection," Technology, Inc., San Antonio, Texas. Quarterly Progress Report No. 2, NASA Contract NAS 2-5062.
8. Orne, D. and Liu, Y. K., (1971), "A Mathematical Model of Spinal Response to Impact," J. Biomechanics 4:49-72.
9. Pontius, U. R., Liu, Y. K. and Van Buskirk, W. C., (1972), "The Effect of the Cervical Neuromusculature on the Dynamics of Whiplash," Proc. of 25th Annual Conf. on Engr. in Med. & Biology, Bal Harbour, FA.
10. Sanford, R. L. and Kellet, G. L., (1966), "A Technical Review and Evaluation of a Proposed Lumbar Pad for U. S. Navy Configuration of MK-H5/H7F-1 Ejection Seats: Phase I-MK-H5," U. S. Naval Air Engineering Center, Report NAEC-ACEL-538.
11. Schane, W. P., Littel, D. E. and Moultrie, C. G., (1969), "Selected Anthropometric Measurements of 1,640 U. S. Army Warrant Officer Candidate Flight Trainees," U. S. Army Aeromedical Research Laboratory, Report No. 69-2.

12. Shannon, R. H., (1970), "Analysis of Injuries Incurred During Emergency Ejection - Extraction Combat and Noncombat," Aerospace Med. 41:798-802.
13. Snyder, R. G., Chaffin, D. B. and Schutz, R. K., (1971), "Joint Range of Motion and Mobility of the Human Torso," 15th Stapp Car Crash Conf., Coronado, California, ASAE Paper No. 710848.
14. Toth, R., (1967), "Multiple Degree-of-Freedom Nonlinear Spinal Model," Presented 19th Ann. Conf. on Engng in Med. and Biol., San Francisco, California.
15. Vulcan, A. P., King, A. I. and Nakamura, G. S., (1970), "Effects of Bending on the Vertebral Column During +G<sub>z</sub> Acceleration," Aerospace Med. 41:294-300.
16. Walker, L. B., Jr., Harris, E. H. and Pontius, U. R., (1973), "The Determination of Some Physical Properties of Cadaver Head and Neck," Proc. 17th Stapp Car Crash Conf., Oklahoma City, Oklahoma.
17. Yamada, H., (1970), Strength of Biological Materials, F. Gaynor Evans, editor, The Williams and Wilkins Co., Baltimore, Maryland.

Unclassified

Security Classification

DOCUMENT CONTROL DATA - R & D		
<i>(Security classification of title, body of abstract and indexing annotation must be entered when the overall report is classified)</i>		
1. ORIGINATING ACTIVITY (Corporate author) US Army Aeromedical Research Laboratory Fort Rucker, Alabama		2a. REPORT SECURITY CLASSIFICATION Unclassified
		2b. GROUP
3. REPORT TITLE  THE EFFECTS OF INITIAL SPINAL CONFIGURATION ON PILOT EJECTION		
4. DESCRIPTIVE NOTES (Type of report and inclusive dates) Paper for publication		
5. AUTHOR(S) (First name, middle initial, last name) Y. King Liu Uwe R. Pontius Ronald R. Hosey		
6. REPORT DATE October 1973	7a. TOTAL NO. OF PAGES 44	7b. NO. OF REFS 17
8a. CONTRACT OR GRANT NO.  b. PROJECT NO. 3AO 6211 OA 819  c.  d.	9a. ORIGINATOR'S REPORT NUMBER(S)  74-6	
9b. OTHER REPORT NO(S) (Any other numbers that may be assigned this report)		
10. DISTRIBUTION STATEMENT  This document has been approved for public release and sale; its distribution is unlimited.		
11. SUPPLEMENTARY NOTES	12. SPONSORING MILITARY ACTIVITY US Army Medical R&D Command Washington, DC 20314	
13. ABSTRACT  The effect of initial spinal alignment on the location and magnitude of maximum vertebral stress during ejection was studied using the Orne-Liu discrete parameter model of the spine. Face curtain, shoulder harness, and seat back restraints were added to the model as linear springs. Spinal alignment data used were from x-rays of a 5th, 40th, and 95th percentile (sitting height) man seated in the MK-J5(D) ejection seat under static conditions. Maximum normal stresses were shown to occur at L1(5th), T12(40th) and T9(95th) with face curtain and shoulder harness restraint. These locations correspond almost exactly to the predictions of injury based on static observations of the curvature of the initial configuration of the pilot's spine. Inclusion of posterior-anterior seat back support decreased maximum stresses as did the use of an improved lumbar pad which placed the lower spinal column in extension. Failure to utilize the face curtain restraint gave rise to large normal stresses in the upper thoracic column. Results indicated that a state of nearly uniform axial stress exists in the column during ejection and thus the location of maximum bending stress dictates the spinal location of the maximum normal stress. Hence, initial spinal alignment, in terms of the curvature of the column, is a major determinant of the location and magnitude of maximum normal stress for a given set of restraints.		

DD FORM 1473  
NOV 66

REPLACES DD FORM 1473, 1 JAN 64, WHICH IS OBSOLETE FOR ARMY USE.

Unclassified

Security Classification

Unclassified

Security Classification

14. KEY WORDS	LINK A		LINK B		LINK C	
	ROLE	WT	ROLE	WT	ROLE	WT
biomechanics pilot ejection spinal injury spinal alignment ejection seat lumbar pad						

Unclassified

Security Classification